View metadata, citation and similar papers at core.ac.uk
brought to you by CORE
provided by NASA Technical Reports Server

Atmospheric Chemical Transport Based on High Resolution Model - Derived Winds: A Case Study

John R. Hannan[1]
Henry E. Fuelberg[1]
Anne M. Thompson[2]
George Bieberbach Jr.[1]
Richard D. Knabb[1]
Yutaka Kondo[3]
Bruce E. Anderson[4]
Edward V. Browell[4]
Gerald L. Gregory[4]
Glen W. Sachse[4]
Hanwant B. Singh[5]

[1]Department of Meteorology, Florida State University, Tallahassee, FL
[2]NASA Goddard Space Flight Center, Greenbelt, MD
[3]Solar-Terrestrial Lab, Nagoya University, Toyokawa, Japan
[4]NASA Langley Research Center, Hampton, VA
[5]NASA Ames Research Center , Moffett Field, CA

Submitted to

Journal of Geophysical Research
SONEX Special Section
February 1999

Corresponding author:
Henry E. Fuelberg
Department of Meteorology
Florida State University
Tallahassee, FL 32306-4520
fuelberg@met.fsu.edu

Abstract

Flight 10 of NASA's Subsonic Assessment (SASS) Ozone and Nitrogen Oxide Experiment (SONEX) extended southwest of Lajes, Azores. A variety of chemical signatures were encountered. These signatures are examined in detail, relating them to meteorological data from a high resolution numerical model having horizontal grid spacing of 30 and 90 km and 26 vertical levels. The meteorological output at hourly intervals is used to create backward trajectories from the locations of the chemical signatures.

Four major categories of chemical signatures are discussed—stratospheric, lightning, continental pollution, and a transition layer. The strong stratospheric signal is encountered just south of the Azores in a region of depressed tropopause height. Three chemical signatures at different altitudes in the upper troposphere are attributed to lightning. Backward trajectories arriving at locations of these signatures are related to locations of cloud-to-ground lightning. Results show that the trajectories pass through regions of lightning 1-2 days earlier over the eastern Gulf of Mexico and off the southeast coast of the United States. The lowest leg of the flight exhibits a chemical signature consistent with continental pollution. Trajectories arriving at this signature are found to pass over the highly populated Northeast Corridor of the United States. Surface based pollution apparently is lofted to the altitudes of the trajectories by convective clouds along the East Coast that did not contain lightning. Finally, a chemical transition layer is described. Its chemical signature is intermediate to those of lightning and continental pollution. Trajectories arriving in this layer pass between the trajectories of the lightning and pollution signatures. Thus, they probably are impacted by both sources.

1. Introduction

NASA's Subsonic Assessment (SASS) Ozone and Nitrogen Oxide Experiment (SONEX) was conducted over the North Atlantic Flight Corridor (NAFC) during Fall 1997 to study the effects of subsonic aircraft emissions on the atmospheric chemistry of the upper troposphere and lower stratosphere. During the sixteen flights comprising the SONEX field phase, NASA's instrumented DC-8 aircraft collected *in situ* high resolution chemical data throughout the NAFC and surrounding areas. *Singh et al.* [this issue] give a comprehensive overview of the SONEX program.

SONEX Flight 10 on October 29, 1997 was a tropical survey originating at Lajes, Terceira Island, Azores (38.7°N, 27.1°W). The flight track was oriented northeast to southwest, reaching a southwestern terminus near 19.9°N, 37.1°W (Figure 1). A stack maneuver of four legs was performed between the southernmost latitude and ~25°N to sample chemical characteristics at multiple levels. Although the goal of Flight 10 was to sample clean, subtropical air exhibiting minimal continental, convective, and aircraft influence, complex chemical signatures from a variety of sources actually were encountered.

Insight into the transport history and origins of air parcels can be gained by relating meteorological data to chemical data. Species-species correlations are useful since they can indicate the types of atmospheric processes that air samples have experienced, e.g., convection, pollution, mixing, and photochemical reactions [*Davis et al.*, this issue, *Thompson et al.*, this issue a]. Trajectory calculations can indicate possible source regions, transport paths, and age of the air [e.g., *Board et al.*, 1999].

Origins and transport paths of atmospheric chemicals over the North Atlantic Ocean are not easily investigated. This is due to the sparsity of meteorological data over oceanic

regions, as well as the vast distances that air parcels can travel over short periods of time in the mid-latitudes. Transport paths and consequently, the chemical composition of air in this region can vary greatly, particularly during the cool season due to strong winds and high amplitude flow patterns.

This research relates observed chemical signatures during SONEX Flight 10 to high-resolution numerically derived meteorological data. Our objective is to understand the chemical signatures by determining source regions and transport paths of the air parcels that were sampled. We use the National Center for Atmospheric Research (NCAR)/Penn State Fifth Generation Mesoscale Model (MM5) [*Grell et al.*, 1994] to create a high resolution three dimensional set of meteorological data. Backward trajectories arriving at locations of the chemical signatures then are calculated using the model-derived winds. Finally, the trajectory paths are related to meteorological and/or anthropogenic chemical sources.

We believe that our high resolution MM5-derived meteorological data (30 or 90 km, hourly) provide a better representation of actual wind regimes and, consequently, more accurate trajectories than is possible using global gridded analysis (typically 110 km, 6-hourly). This improved resolution is important since trajectories are highly sensitive to small errors in both wind direction and speed as well as the temporal frequency of the wind data [*Doty and Perkey*, 1992]. Other studies that have used high resolution numerically-derived meteorological data to compliment the synthesis of high resolution chemical data include *Chatfield et al.* [1996, this issue], *Pickering et al.* [1996, this issue], *Liu et al.* [1996], and *Wang et al.* [1996].

2. Data and Methodology

2.1 Meteorological Data

We employed a two-way interactive nested configuration for the non-hydrostatic MM5 simulations (Figure 2). The coarse outer grid extended far beyond the SONEX region, covering most of North America and Europe, to reduce the effects of boundary errors [*Warner et al.*, 1997]. The horizontal spacing of the coarse grid was 90 km, with 147 grid points in the east to west direction and 87 grid points south to north. The higher resolution inner grid, centered over the path of Flight 10, had a horizontal spacing of 30 km. This grid contained 136 points east to west and 166 grid points south to north. Both domains utilized 26 sigma levels in the vertical that were relatively closely spaced near the tropopause (~20 hPa separation). The Grell cumulus scheme [*Grell*, 1993] and the Blackadar planetary boundary layer scheme [*Zhang and Anthes*, 1982] were chosen as the model physics parameterizations.

The MM5 was initialized with a gridded data set prepared by the European Centre for Medium-Range Weather Forecasting (ECMWF) [*Bengtsson*, 1985, *Hollingsworth et al.*, 1986]. The resolution of these data was 2.5° by 2.5° in the horizontal with 15 isobaric levels in the vertical between 1000 and 10 hPa. Boundary conditions at subsequent times also were obtained from the ECMWF data. Sea surface temperatures were taken from a data set provided by the National Center for Environmental Prediction (NCEP). The 67 hour simulation on the 90 km domain began at 0000 UTC October 27, 1997 and ended at 1900 UTC October 29. The simulation for the 30 km domain was started at 0000 UTC October 28 and also ended at 1900 UTC October 29. Model data for the first 12 hours of each simulation were not utilized to allow for a sufficient "spin up" period.

Trajectories were calculated from the MM5 data using the kinematic method. That is, air parcels were advected using only the three dimensional wind field, without employing the isentropic assumption. The wind data at 26 sigma levels were interpolated to 241 equally spaced isobaric levels using a cubic spline procedure. Linear interpolation provided values between levels as well as at 5-minute time steps. *Fuelberg et al.* [1996] give further details about the trajectory model as well as a comparison between the kinematic and isentropic methods.

Limitations of trajectories include incorrect placement of meteorological features by the input analyses. This is of particular concern over oceanic regions, such as the SONEX domain, where meteorological data are relatively sparse. However, numerical models such as the MM5 can generate the features that may be lacking in the coarser input data. Trajectories also are subject to the resolution of the wind data, since features of sufficiently small time or space scales will not be resolved [*Doty and Perkey*, 1992]. Resolution in our two domains was 1 hour and either 30 or 90 km. Thus, individual convective elements (e.g., their updrafts) still are not resolved. However, the effects of the convection are depicted at the scale of the grid. Finally, numerical limitations of the kinematic model itself affect overall trajectory accuracy [*Stohl et al.*, 1995]. The kinematic method has been widely used in many meteorological/chemical applications [*Draxler*, 1991, *Doty and Perkey*, 1993, *Krishnamurti et al.*, 1993, *Chatfield et al.*, 1996, *Garstang et al.*, 1996, and *Bieberbach et al.*, this issue].

Arrival locations for the backward trajectories were at 1-minute intervals along the flight path. Trajectory arrival times were the hour closest to the actual times of the *in situ* chemical observations. The trajectories were derived from a combination of the 30 and 90

km MM5 wind data. Specifically, the first 19-29 hours from the flight track were calculated from the 30 km (innermost) data grid, depending on time of arrival at the boundary of the 30 km domain. The earlier 24-34 hours were calculated using the 90 km data.

Locations of convection were determined using cloud-to-ground lightning data from the National Lightning Detection Network (NLDN) and Long Range Field (LRF) [*Cummins et al.*, 1998]. GOES-8 infrared imagery also was employed.

2.2 Chemical Data

The chemical data used in this study were taken from a 1 minute merged data set prepared at Harvard University. This data set contains 1-minute averages of all chemical, meteorological, and position data recorded during the flight, as well as model-derived values of certain chemical species. *Singh et al.* [this issue] describe the chemical measurements in detail.

3. Meteorological Conditions

High amplitude flow patterns dominated the SONEX period, including the day of Flight 10 [*Fuelberg et al.*, this issue]. Figure 3 contains winds and potential vorticity at 250 hPa (~10.5 km) on 1200 UTC October 29 derived from the 1° x 1° ECMWF data (panels a,b) and the 90 km and 30 km MM5 simulations (panels c,d).

Circulation patterns from the MM5 at 90 km resolution (Figure 3c) agree closely with those from ECMWF (Figure 3a), particularly the trough/ridge system near the NAFC. The cut-off low near the Azores also is similarly placed, although wind speeds from the MM5 are slightly greater (~10 m s^{-1}) than those in the ECMWF analyses. The departure site of Flight 10 (the Azores) was nearly coincident with this cyclone that had been drifting

slowly eastward after becoming detached from the main flow. The long wave trough and ridge axes (dashed lines) located south and west of the low, respectively, also are depicted similarly. The relatively deep trough south of Newfoundland was oriented over the southeastern United States two days prior to the flight. This system and its associated frontal boundaries produced extensive lightning from the central Gulf of Mexico to the coastal waters off the eastern United States. The two versions of the jet stream exhibit only slight differences in placement and wind speed.

Potential vorticity (PV) (Figure 3b,d) provides a rigorous comparison between the ECMWF and MM5 data since PV requires derivatives of temperature and the horizontal wind components. The two versions of PV at 250 hPa exhibit close agreement, i.e., major features are similarly placed with only minor differences in magnitude. The MM5 generates an 11 PVU (1 PVU = 1×10^{-5} K mb^{-1} s^{-1}) maximum near the Azores at 30 km resolution compared to the 12 PVU maximum indicated by the ECMWF analysis. The pattern of isopleths indicates that the MM5 better resolves this tropopause undulation. The two PV maxima to the northeast and northwest of the main feature also are comparably represented in terms of magnitude, with maximum variations of only 1 PVU.

Although only two parameters at 250 hPa are described here, we have compared the MM5 and ECMWF versions of many meteorological variables at various altitudes. Close agreement is found in all cases. Therefore, we believe that the MM5 simulation can be used confidently to understand the chemical signatures observed during Flight 10. Unless otherwise noted, future meteorological analyses will be derived from the MM5.

4. Results

Results show that the complex chemical signatures observed during Flight 10 can be directly linked to the meteorological features described in Section 3. The stratospheric influence during the flight was among the greatest of the entire SONEX mission [*Thompson et al.*, this issue a]. The convective influence also was pronounced [*Chen et al.*, this issue, *Davis et al.*, this issue, *Snow et al.*, this issue, and *Thompson et al.*, this issue a], and a moderate amount of continental pollution was encountered.

Three distinct chemical signatures were observed during Flight 10, and correlations between NO_y and CO and between NO_y and CN are useful in differentiating between them e.g., *Thompson et al.* [this issue, a], *Jaeglé et al* [1996]. Figure 4 shows scatter diagrams of these three species during the flight. Stratospheric air is easily distinguished from lightning influenced or continental air since NO_y is anti-correlated with both CO and CN in the stratosphere. Large NO_y associated with large CO and large CN indicates lightning. Conversely, moderate NO_y with moderate CO and CN denotes continental influence. Stratospheric and tropospheric regimes can be distinguished by the probability distribution of ozone mixing ratio (Figure 5). Although most ozone measurements during Flight 10 are less than 100 ppbv, numerous samples exceed the customary 100 ppbv stratospheric threshold, with some approaching 450 ppbv.

Figures 6 and 7 are time series of selected chemical species measured along the path of Flight 10. Chemical signatures are denoted along the tops of the figures—two encounters of stratospheric air, three lightning signatures, one signature representing continental pollution, and a broad transition region along two flight legs. The bottom plot of each figure depicts flight altitude. Plate 1 shows the altitude and latitude of the flight and the

chemical signatures. The following sections describe chemical characteristics and transport paths associated with each signature. The two stratospheric portions of the flight (STR) are examined first. Next, we explore the three signatures associated with lightning (LT1, LT2, and LT3) and the pollution signal (POL). Finally, the transition region (TRS) is examined.

4.1 Stratospheric Signature

Well defined stratospheric air is encountered during Flight 10. Stratospheric penetration occurs on both the outbound and inbound legs when the DC-8 passes through the cutoff low near the Azores (Figure 3). During the outbound penetration, the stratospheric signal occurs between 1128-1214 UTC (Plate 1, Figures 6,7), i.e., after the aircraft ascends to 10.1 km (267 hPa). Values of O_3 and NO_y increase sharply to ~250 ppbv and 1000 pptv, respectively. Conversely, values of CO (< 40 ppbv), ultrafine CN (< 1000 cm^{-3}), and water vapor (< 100 ppmv) show dramatic decreases, while NO (< 100 pptv) and PAN (~40 pptv) decrease to a small fraction of NO_y. Penetration during the return leg occurs at a higher altitude than before (11.9 km (202 hPa) between 1725-1830 UTC), producing an even greater value of ozone (> 400 ppbv).

The tropopause is relatively low near the cutoff low. This depression is depicted in the cross section of PV (Figure 8). If we assume that the stratospheric threshold is 3.0 PVU [*Fuelberg et al.*, this issue], the lowest altitude of the stratosphere is ~7 km. The Dial (Differential absorption lidar) [*Browell,* 1989, 1991] ozone image (Plate 2) shows the downward protrusion of ozone rich stratospheric air. Specifically, O_3 > 100 ppbv extends to ~6 km during the return portion of the flight (right side of figure), with enhanced ozone (> 80 ppbv) reaching nearly 3 km. Backward trajectories arriving at the stratospheric portion of the flight (not shown) remain at stratospheric altitudes throughout their 2-day histories.

4.2 Lightning Signatures

Three regions of enhanced NO of varying intensity and duration are attributed to lightning. Trajectory analyses will show that each of these regions is associated with an extensive area of lightning that occurred along the East Coast of the United States 1 to 2 days prior to the flight.

The longest chemical signature attributed to lightning (LT1) occurs from 1404 to 1452 UTC (Figures 6,7). One should note that the bounds of LT1 encompass the entire flight leg at 9.5 km (292 hPa, Plate 1). The chemical signature of LT1 includes enhanced mixing ratios of NO (300-500 pptv), NO_y (500-1000 pptv), and water vapor (200-300 ppmv), as well as enhanced ultrafine CN (10,000-17,000 cm^{-3}). However, CO is slightly reduced (~80 ppbv).

Figure 9 shows a horizontal plot of backward trajectories arriving at locations comprising LT1. The trajectories pass over the Florida peninsula approximately two days prior to arrival, travel offshore of the Carolinas as they head northeast toward Newfoundland, and then turn southeast toward the flight track. To determine the extent to which parcels comprising LT1 were exposed to lightning, we superimpose trajectory and NLDN cloud-to-ground lightning data over 3-hour intervals. Although intracloud lightning also produces nitrogen oxides, no data about its occurrence was available at the needed resolution. The trajectories experience two major encounters with cloud-to-ground lightning. The first occurs between 1200-1800 UTC October 27 (Plate 3) as they pass through the eastern Gulf of Mexico into Florida. The greatest exposure occurs between 1200-1500 UTC when the trajectories are nearly coincident with a concentrated area of cloud-to-ground flashes. Heights of individual trajectories during this encounter (47-51 hours back in Figure 10) vary

considerably, with the highest trajectories near 9.8 km and the lowest near 6.0 km. Satellite imagery (not shown) indicates cloud top temperatures in this area that correspond to heights of ~9-12 km (~300 hPa to 200 hPa). *Pickering et al.* [1996] found that maximum convective outflow occurred near the tops of clouds that were investigated over Brazil.

The trajectories comprising LT1 experience a second major encounter with lightning approximately 18 hours after the first (Plate 3). This occurs between 0600-0900 UTC October 28 as the trajectories exit the northern edge of the flash region. Maximum cloud heights in this area (29-33 hours back in Figure 10) are ~12 km (200 hPa), while trajectory heights have risen to ~7.0-11.5 km (213-473 hPa).

It is informative to examine lightning signature LT2 in the context of the LT1 signature just described. LT2 is brief, extending only from 1322-1331 UTC (Figures 6,7). It occurs while the DC-8 ascends (Plate 1) from a leg at 8.8 km (319 hPa) to a leg at 10.7 km (243 hPa). Specifically, LT2 begins when the DC-8 ascends through the altitude of LT1 (9.5 km, 292 hPa) in a location directly above LT1. Values of NO, NO_y, CN, CO, and water vapor for LT2 are very similar to those observed during LT1. In addition, the trajectories arriving at LT2 (Plate 4) have lightning encounters that are very similar in both time and space to those of the LT1 trajectories (Plate 3). Thus, LT2 appears to be a quick sampling of the same lightning event that produces LT1.

The LT2 signature ends part way through the 10.7 km leg at ~1330 UTC (Figures 6,7, Plate 1). This corresponds to an increase in O_3 to ~80 ppbv, and a decrease in H_2O to values similar to those encountered in the stratosphere. The DIAL image (Plate 2) indicates a downward protrusion of relatively large O_3 in the region, and the horizontal analysis of PV (Figure 3b,d) shows that this location (~23 N, 35 W) lies along a narrow band of enhanced

PV. A time series of flight level PV (Figure 9 in Fuelberg et al. [this issue]) indicates that values in this area increase to ~2.0 PVU. These factors suggest that the region exhibits a weak stratospheric influence. The only counter indication is that CO does not show the decrease that is expected of stratospheric air.

The third lightning episode (LT3) occurs between 1646-1716 UTC as the DC-8 heads back to the Azores after the stack maneuver. The signature begins at an altitude of 10.3 km (245 hPa) while the aircraft is ascending from the 5.8 km (486 hPa) leg to the 11.9 km (202 hPa) leg (Plate 1). The signal continues along the 11.9 leg until the second stratospheric penetration occurs (Section 4.1). The chemical signature of LT3 is the most intense of the three lightning events (Figures 6,7). LT3 exhibits the greatest NO (1500 pptv) and NO_y (2000 pptv) of the entire flight. Values of ultrafine CN (30,000 cm^{-3}) also are greatest in this segment, while CO is relatively small (~80 ppbv).

Trajectories arriving along the level leg of LT3 at 11.9 km are shown in Figure 11. Their locations are not greatly different from those comprising LT1 (Figure 9). However, even these slight differences cause the LT3 trajectories to coincide more closely with the cloud-to-ground lightning locations, and for a longer period of time, than do those of the other lightning signatures. These lightning encounters are shown in Plate 5. The event begins near 1500 UTC October 27 as the first trajectories arrive at the southwestern edge of an extensive line of intense convection over the Gulf of Mexico. This encounter region, immediately north of the Yucatan Peninsula, contains the highest cloud tops of the entire line (> 12 km, < 200 hPa). At this initial time, only the southernmost trajectories coincide with the region of cloud-to-ground lightning. However, as the trajectories move eastward, their horizontal separation decreases, leading to a greater number of trajectory/lightning

encounters. Thus, between 1800-2100 UTC (Plate 5), a significantly greater number of trajectories are co-located with lightning. This first encounter ends at ~2100 UTC October 27, and over the next 12 hours (not shown), the number of lightning flashes decreases greatly. The trajectories pass over South Florida and emerge over the coastal waters of the Atlantic during this period.

Cloud-to-ground lightning flashes increase dramatically over the western Atlantic Ocean after 0600 UTC October 28 (not shown), and the eastward moving trajectories pass through the southern part of this region between 0900-1500 UTC October 28 (Plate 5). One should note that almost all of the trajectories pass through the area of intense lightning at some time during this period. Over this six hour span, trajectory heights remain virtually constant at near 12 km (200 hPa, not shown), corresponding approximately to cloud top level.

To summarize, the strength of the LT3 chemical signature (Figures 6,7) apparently is due to the long period over which its trajectories are exposed to extensive lightning. This exposure for LT3 is greater than observed with the two other weaker lightning signatures (LT1-2).

It should be noted that the high-resolution MM5 wind data were valuable for computing the trajectories arriving at LT3. For example, trajectories calculated from ECMWF data, where resolution (6-hourly, 1degree) is coarser than the MM5, were not coincident with the observed lightning flashes at any time during their 2-day histories (not shown).

Finally, a brief chemical "spike" occurs at ~1220 UTC at the southern end of the 10.1 km flight leg (Figures 6,7, Plate 1). It is located just south of the stratospheric region,

near 32°N. The spike is characterized by slightly enhanced values of NO (~250 pptv), NO_y (~600 pptv), and ultrafine CN (~8000 cm^{-3}). This signature also is consistent with a brief lightning encounter. Its altitude is between those of LT1-3. Thus, results indicated that the layer between ~9-12 km located south of the stratospheric region is characterized by a lightning signature.

4.3 Pollution Signature

The pollution signature (POL) begins when the DC-8 descends to its lowest altitude of the flight (5.8 km, 486 hPa) (Figures 6,7, Plate 1). It occurs during the entire length of this leg, from ~1528-1646 UTC (20°-28°N). Several species exhibit moderately enhanced values, including PAN (70-120 pptv), H_2O (500-1500 ppmv), and O_3 (80 ppbv) in Figures 6,7 and C_2H_2(100-140 pptv), H_2O_2 (250-450 pptv), and CH_3OOH (75-150 pptv) (not shown). Values of NO and CN are not enhanced.

Horizontal plots of the trajectories comprising POL are shown in Figure 12. Although their basic orientation is similar to those seen for previous signatures, the important difference is that these trajectories pass very near the heavily populated Northeast Corridor of the United States. Plate 6 focuses on the trajectories between 1500-2100 UTC October 27 when they pass along the East Coast. One should note that there are virtually no encounters between the trajectories and cloud-to-ground lightning, i.e., the trajectories pass west of the lightning. This is consistent with the chemical signature. On the other hand, satellite imagery (Plate 6) indicates that the trajectories do pass near relatively deep clouds that do not contain cloud-to-ground lightning. Cloud locations at 2045 UTC are especially interesting (Plate 6c), i.e., a band of rain showers parallels the coast from North Carolina to Cape Cod.

Coldest cloud top temperatures range from -35° to -45°C, corresponding to heights of ~7.5-9.5 km. The median trajectory altitude in this region is ~8.6 km (between 36-42 hours back in Figure 13). Since this area is west of a cold front that is located offshore over the Atlantic, low level winds are from the northwest (not shown). Thus, it appears that surface based pollution from the Northeast Corridor is transported at low levels toward the line of convection, transported aloft by the convective updrafts, and then carried horizontally to the location of the POL signature.

4.4 Transition Layer

The layer between ~7-9 km appears to be a transition region (TRS). It is sampled during two flight legs, i.e., first at 8.8 km (320 hPa) between 1245-1319 UTC, and again at 7.6 km (376 hPa) between 1453-1526 UTC (Plate 1). A chemical "spike" is evident along the 8.8 km leg (indicated by an ellipse in Plate 1 and an arrow in Figures 6,7). The signature occurring at ~1310 UTC is characterized by the following values: NO (90 pptv), NO_y (300 pptv), and ultrafine CN (5000 cm^{-3}). Although these values are only slightly enhanced compared to the background, they are consistent with a weak lightning signature.

Plate 7 shows that the trajectories comprising this signature experience only a slight encounter with cloud-to-ground lightning between 2100 UTC October 27 to 0300 UTC October 28 as they exit the coastal waters of the United States to the northeast. There are no close encounters during the periods that are not shown. These trajectories originate over Florida 49 hours earlier and then pass just south of Newfoundland before arriving at the flight track from the northwest (not shown). At the times when trajectory paths coincide with

lightning locations, trajectory altitudes (not shown) are ~5.7-6.2 km (~450-490 hPa), while satellite derived cloud top temperatures indicate heights near ~7-9 km (~300-400 hPa).

The 8.8 km flight leg containing the lightning "spike" is below the legs containing the major lightning signatures (LT1-3, Plate 1). And, trajectories arriving at the level of the spike pass over the coastal waters of the East Coast at lower altitudes than those arriving near LT1-3 (not shown). These lower levels appear to be below the main outflow of the extensive storms producing the intense cloud-to-ground lightning. Thus, the DC-8 may be sampling outflow from intermittent lower level lightning producing storms. This hypothesis is difficult to verify with the hourly satellite-derived cloud top data that are available.

The lower altitude transition signature (TRS) begins at ~1453 UTC when the DC-8 descends to 7.6 km (376 hPa) (see Figures 6,7, Plate 1). The signature lasts ~30 minutes (until 1526 UTC) when the DC-8 descends to its lowest leg containing POL. Plate 1 shows that this 7.6 km leg lies between the altitude legs containing LT1 (9.5 km) and POL (5.8 km). The chemical signature at 7.6 km is intermediate to those above and below. For example, note the values of NO (~100 pptv), NO_y (~400 pptv), ultrafine CN (~8000 cm^{-3}), PAN (~60 pptv), water vapor (200-300 ppmv), and hydrogen peroxide (H_2O_2, ~100 pptv, not shown).

Horizontal locations of trajectories arriving along the 7.6 km TRS leg are shown in Figure 14. One should note that paths along the East Coast are intermediate to those of LT1 (Figure 9), located directly above (at 9.5 km), and POL (Figure 12), located directly below (at 5.8 km). The LT1 trajectories are farthest offshore, encountering extensive cloud-to-ground lightning (Plate 3). Conversely, the POL trajectories are farthest west, avoiding virtually all of the lightning (Plate 6), but encountering continental pollution that was carried offshore by northwesterly winds behind a cold front. The intermediate TRS trajectories

experience some lightning encounters (not shown), but also appear to carry a pollution signature. The altitudes of the trajectories, when passing along the East Coast (Figure 15), support this hypothesis. One should note the wide range of trajectory altitudes (5.5-10 km, 500-275 hPa) during passage from Cape Hatteras to east of Cape Cod between 36-42 hours prior to arriving at the DC-8. This contrasts with the more narrow range of altitudes exhibited by the LT1 and POL trajectories in this region (Figures 10, 13). This range of altitudes should encompass outflow from deep convection having extensive lightning as well as more shallow clouds with little or no lightning.

The background chemical signature along the 8.8 km TRS leg near 1230 UTC (Figures 6,7, Plate 1) is not identical to that along the lower 7.6 km TRS leg. The upper TRS leg also contains the chemical spike that was attributed to a brief lightning encounter. These chemical differences are expected in a transition layer that is not fully mixed.

5. Summary and Conclusions

Flight 10 of NASA's Subsonic Assessment (SASS) Ozone and Nitrogen Oxide Experiment (SONEX) originated in Lajes, Azores (38.7°N, 27.1°W) and extended southwest to 19.9°N, 37.1°W. A variety of chemical signatures were encountered during the flight. A stack maneuver along the southern half of the flight track provided samples at four different altitudes, i.e., 10.7, 9.5, 7.6, and 5.8 km. The horizontal length of these flight legs was relatively short, only ~400-800 km. In this research we have examined the chemical signatures in detail, relating them to high resolution meteorological data from a mesoscale numerical model.

The National Center for Atmospheric Research (NCAR)/Penn State Fifth Generation Mesoscale Model (MM5) was used to create a high resolution three dimensional meteorological data set. The model was configured with two way interactive nesting, i.e., with a coarse (90 km) outer grid and a finer (30 km) internal grid. Each domain contained 26 vertical levels. Analyses from the MM5 simulation agreed closely with global analyses. The MM5 data were available at hourly intervals and then used to create backward trajectories from the locations of the chemical signatures. We believe that the MM5-derived meteorological data provided a better representation of actual wind regimes and, consequently, more accurate trajectories than possible using global gridded analysis (typically 110 km, 6-hourly). This improved resolution is important since trajectories are very sensitive to slight errors in both wind direction and speed as well as the temporal frequency of the wind data.

Four major categories of chemical signatures were discussed—stratospheric, lightning, continental pollution, and a transition layer. The strong stratospheric signal was encountered just south of the Azores. Values of O_3 were greatly enhanced, while values of CO and water vapor were very small. The tropopause was relatively low in the region, extending down to ~6 km, due to a nearby closed low pressure circulation.

Three chemical signatures were attributed to lightning. These signatures were located south of the lowered stratospheric region at relatively high altitudes (11.9, 10.7 and 9.5 km). Two of the signatures occurred during the stack maneuver. Their chemical characteristics included enhanced values of NO, NO_y, and water vapor, as well as enhanced ultrafine CN. Backward trajectories arriving at locations of the chemical signatures were related to locations of cloud-to-ground lightning. Results showed that the trajectories had

passed over regions of lightning located over the eastern Gulf of Mexico and off the southeast coast of the United States 1-2 days earlier. Two additional lightning signatures (the "spikes") were observed during legs at 8.8 and 10.1 km.

The lowest leg of the stack maneuver (5.8 km) exhibited a chemical signature consistent with continental pollution. Species that were enhanced included PAN, water vapor, O_3, C_2H_2, H_2O_2, and CH_3OOH. Trajectories arriving at the pollution signature had passed over the highly populated Northeast Corridor of the United States. Since they passed to the west of the region of lightning that was farther offshore, no lightning signature was indicated. Surface based pollution apparently was lofted to the altitudes of the trajectories by convective clouds along the East Coast that did not contain lightning.

Finally, a transition layer was detected along two flight legs between ~7-9 km. The chemical signature at 7.6 km was intermediate to signatures located at higher and lower flight legs. Species having intermediate values included NO, NO_y, CN, PAN, water vapor, and hydrogen peroxide. The lightning signature was located directly over the 7.6 km leg at an altitude of 9.5 km, while the pollution signature was located directly below at 5.8 km. Trajectories arriving in this region had passed over locations off the East Coast that were between those of the lightning and pollution signatures. Thus, they probably were impacted by both lightning and pollution. These trajectories exhibited a wide range of altitudes when passing over the region of influence. A second leg of transition was located at 8.8 km. The chemical signature along this leg was not as pronounced as that at 7.6 km.

In summary, the results show that high resolution numerical modeling can provide meteorological data that are useful for understanding complex chemical signatures. This capability was especially evident during the aircraft's stack maneuver, when four different

chemical signatures were co-located at different altitudes, i.e., pollution, transition, lightning, and stratospherically influenced.

Acknowledgments

We appreciate the many helpful conversations with various members of the SONEX Science Team, especially Ken Pickering, Doug Davis, and Julie Snow. Jim Crawford provided the hourly NLDN data. This research was sponsored by the NASA Atmospheric Effects of Aviation Program.

References

Bengtsson, L., Medium-range forecasting--The experience of ECMWF, *Bull. Am. Meteorol. Soc.*, 66, 1133-1146, 1985.

Bieberbach, G., H.E. Fuelberg, A.M. Thompson, A. Schmitt, J.R. Hannan, Y. Kondo, and R.D. Knabb, Mesoscale numerical simulations of air traffic emissions over the North Atlantic during SONEX flight 8: A case study, *J. Geophys. Res.*, this issue.

Board, A.S., H.E. Fuelberg, G.L. Gregory, B.G. Heikes, M.G. Schultz, D.R. Blake, J.E. Dibb, S.T. Sandholm, and R.W. Talbot, Chemical characteristics of air from differing source regions during PEM-Tropics A, *J. Geophys. Res.*, in press, 1999.

Browell, E.V., Differential absorption lidar sensing of ozone, *Proc. IEEE*, 77, 419-432, 1989.

Browell, E.V., Ozone and aerosol measurements with an airborne lidar system. *Opt. Photonics News*, 2, No. 10, 8-11, 1991.

Chatfield, R.B., J.A. Vastano, H.B. Singh, and G.W. Sachse, A general model of how fire emissions and chemistry produce African/oceanic plumes (O3, CO, PAN, smoke) in TRACE A, *J. Geophys. Res.*, 101, 24279-24306.

Chatfield, R.B., N. Blake, D.R. Blake, Y. Kondo, G.L. Gregory, B.E. Anderson, and H.B. Singh, A statistical analysis of the sources for NO_x observed in the Atlantic free troposphere during the SONEX period: Integrating models with observations, *J. Geophys. Res.*, this issue.

Chen, G.D., D.D. Davis, D.R. Blake, W. Brune, G.W. Sachse, Y. Kondo, A. Viggiano, B.E. Anderson, and F. Arnold, A case study of SONEX flight 10 in the North Atlantic II: Sources and time evolution of H_2SO_4 and SO_4, *J. Geophys. Res.*, this issue.

Cohan, D.S., M.G. Schultz, and D.J. Jacob, Convective injection and photochemical decay of peroxides in the tropical upper troposphere: Methyl iodide as a tracer of marine convection, *J. Geophys. Res.*, in press, 1999.

Cummins, K.L., M.J. Murphy, E.A. Bardo, W.L. Hiscox, R.B. Pyle, and A.E. Pifer, A combined TOA/MDF technology upgrade of the U.S. national lightning detection network, *J. Geophys. Res.*, 103, 9035-9044, 1998.

Davis, D.D, et al., A case study of SONEX flight 10 in the North Atlantic I: Sources and evolution of NO_x and HO_x chemistries, *J. Geophys. Res.*, this issue.

Doty, K.G. and D.J. Perkey, Sensitivity of trajectory calculations to the temporal frequency of wind data, *Mon. Wea. Rev.*, 121, 387-401, 1992.

Draxler, R.R., The accuracy of trajectories during ANATEX calculated using dynamic model analyses versus rawinsonde observations, *J. Appl. Meteorol.*, 30, 1446-1467, 1991.

Fuelberg, H.E., J.R. Hannan, A.M. Thompson, G. Bieberbach Jr., H.B. Selkirk, K.E. Pickering, and D. D. Davis, A meteorological overview of SONEX, *J. Geophys. Res.*, this issue.

Fuelberg, H.E., R.O. Loring Jr., M.V. Watson, M.C. Sinha, K.E. Pickering, A.M. Thompson, G.W. Sachse, D.R. Blake, and M.R. Schoeberl, TRACE A trajectory intercomparison 2. Isentropic and kinematic methods. *J. Geophys. Res.*, 101, 23927-23939, 1996.

Garstang, M., P.D. Tyson, R. Swap, M. Edwards, P. Kallberg, and J.A. Lindesay, Horizontal and vertical transport of air over southern Africa, *J. Geophys. Res.*, 101, 23721-23736, 1996.

Grell, G.A., Prognostic evaluation of assumptions used by cumulus parameterizations, *Mon. Wea. Rev.*, 121, 764-767, 1993.

Grell, G.A., J. Dudhia, and D.R. Stauffer, A description of the fifth-generation mesoscale model (MM5), *Tech. Note, NCAR/TN-398+STR*, 138 pp., Natl. Cent. Atmos. Res., 1994.

Hollingsworth, A., D.B. Shaw, P. Lonnberg, L. Illari, K. Arpe, and A.J. Simmons, Monitoring of observations and analysis quality by a data assimilation system, *Mon. Wea. Rev.*, 114, 861-879, 1986.

Jaeglé, L., D.J. Jacob, Y. Wang, A.J. Weinheimer, B.A. Ridley, T.L. Campos, G.W. Sachse, and D.E. Hagen, Sources and chemistry of NO_x in the upper troposphere over the United States, *Geophys. Res. Lett.*, 25, 1998.

Krishnamurti, T.N., H.E. Fuelberg, M.C. Sinha, D. Oosterhof, E.L. Bensman, and V.B. Kumar, The meteorological environment of the tropospheric ozone maximum over the tropical South Atlantic Ocean, *J. Geophys. Res.*, 98, 10621-10641, 1993.

Lee, D.S., I. Koehler, E. Grobler, F. Rohrer, R. Sausen, Gallardo, L. Klenner, J.J.G. Olivier,

F.J. Dentener, and A.F. Bouwman, Estimates of global NO_x emissions and their uncertainties, *Atmos. Environ.*, 31, 1735-1749, 1997.

Liu, S.C. et al., A model study of tropospheric trace species during PEM-West A: Continental vs marine, *J. Geophys. Res.*, 101, 2073-2086, 1996.

Pickering, K.E., A.M. Thompson, Y. Wang, W.-K. Tao, D.P. McNamara, V.W.J.H. Kirchoff, B.G. Heikes, G.W. Sachse, J.D. Bradshaw, G.L. Gregory, and D.R. Blake, Convective Transport of biomass burning emissions over Brazil during TRACE A, *J. Geophys. Res.*, 101, 23993-24012, 1996.

Pickering, K.E., A.M. Thompson, L. Pfister, T.L. Kucsera, Y. Kondo, G.W. Sachse, B.E. Anderson, and D.R. Blake, Comparison and interpretation of chemical measurements from two SONEX flights over the Canadian Maritimes: Lightning, convection and aircraft signatures, *J. Geophys. Res.*, this issue.

Singh, H.B., A.M. Thompson, and H. Schlager, The 1997 SONEX aircraft campaign: Overview and accomplishments, *J. Geophys. Res.*, this issue.

Snow, J.A., B.G. Heikes, I. Simpson, D.R. Blake, H.B. Selkirk, H.E. Fuelberg, A.M. Thompson, and N. Blake, A comparison of convective tracers during SONEX, *J. Geophys. Res.*, this issue.

Stohl, A., G. Wotawa, P. Seibert, and H. Kromp-Kolb, Interpolation errors in wind fields as a function of spatial and temporal resolution and their impact on different types of kinematic trajectories, *J. Appl. Meteor.*, 34, 2149-2165, 1995.

Thompson, A.M., L.C. Sparling, Y. Kondo, B.E. Anderson, G.L. Gregory, and G.W. Sachse, Fingerprinting NO_x on SONEX: What was the aircraft contribution to NO_x and NO_y?, *J. Geophys. Res.*, this issue a.

Thompson, A.M., L. Pfister, T.L. Kucsera, L.R. Lait, H.B. Selkirk, K.E. Pickering, Y. Kondo, and G.L. Gregory, The Goddard/Ames meteorological support and modeling system during SONEX: Evaluation of analyses and trajectory-based model products., *J. Geophys. Res.*, this issue b.

Wang, Y., W.-K. Tao, K.E. Pickering, A.M. Thompson, J.S. Kain, R.F. Adler, J. Simpson, P. R. Keehn, and G.S. Lai, Mesoscale model simulations of TRACE A and Preliminary Regional Experiment for Storm-scale Operations and Research Meteorology convective systems and associated tracer transport, *J. Geophys. Res.*, 101, 24013-24027, 1996.

Warner, T.T., R.A. Peterson, and R.E. Treadon, A tutorial on lateral boundary conditions as a basic and potentially serious limitation to regional numerical weather prediction, *Bull. Am. Meteorol. Soc.*, 78, 1997.

Zhang, D.-L., and R.A. Anthes, A high-resolution model of the planetary boundary layer sensitivity tests and comparisons with SESAME-79 data, *J. Appl. Meteor.*, 21, 1594-1609, 1982.

Plate Captions

Plate 1. Altitude profile of Flight 10 as a function of latitude. Chemical signatures are indicated by colored segments as follows: Red-stratospheric, blue-lightning, green-transition, and orange-pollution. Lightning signatures within the transition leg and at the end of the stratospheric leg are circled.

Plate 2. Cross section of DIAL-derived O_3 mixing ratio. The O_3 scale (ppbv) and time (UTC) are give at the top while latitude and longitude are given at the bottom. Altitude in kilometers is given along the sides.

Plate 3. Lightning event 1. Three hour trajectory paths are indicated by blue circles. NLDN cloud-to-ground lightning flashes are indicated in red. The time segment is given at the top of each panel.

Plate 4. Lightning event 2. Three hour trajectory paths are indicated by blue circles. NLDN cloud-to-ground lightning flashes are indicated in red. The time segment is given at the top of each panel.

Plate 5. Lightning event 3. Three hour trajectory paths are indicated by blue circles. NLDN cloud-to-ground lightning flashes are indicated in red. The time segment is given at the top of each panel.

Plate 6. a) GOES-8 infrared satellite image at 1445 UTC October 27, 1997.

b) Three hour trajectory paths (blue) and NLDN cloud-to-ground lightning strikes (red) for the period of 1500-1800 UTC October 27, 1997.

c) GOES-8 infrared satellite image at 2045 October 27, 1997.

d) Three hour trajectory paths (blue) and NLDN cloud-to-ground lightning strikes (red) for the period of 1800-2100 UTC October 27, 1997.

Plate 7. Transitional segment. Three hour trajectory paths are indicated by blue circles. NLDN cloud-to-ground lightning flashes are indicated in red. The time segment is given at the top of each panel.

Figure Captions

Figure 1. DC-8 flight track on October 29, 1997.

Figure 2. Domains for the MM5 simulation. The outer perimeter indicates the boundary of the 90 km domain. The inner box represents the area of the 30 km domain. The track of Flight 10 is indicated within the 30 km domain.

Figure 3. a) ECMWF 250 hPa streamlines and isotachs at 1200 UTC October 29, 1997. Wind speeds are contoured at intervals of 10 m s^{-1}.

b) ECMWF 250 hPa potential vorticity at 1200 UTC October 29, 1997. Contours are 1 PVU.

c) MM5 250 hPa streamlines and isotachs at 1200 UTC October 29, 1997. Wind speeds are contoured at intervals of 10 m s^{-1}.

d) MM5 250 hPa potential vorticity at 1200 UTC October 29, 1997. Contours are 1 PVU. The axis of a cross section in Figure 8 is shown.

Figure 4. a) Correlation plot of NO_y (pptv) versus CO (ppbv). The three main signatures of Flight 10 are labeled.

b) Correlation plot of NO_y (pptv) versus the logarithm of ultrafine CN (cm^{-3}). The three main signatures of Flight 10 are labeled.

Figure 5. Probability distribution function of O_3 for Flight 10. Ozone values of 100 ppbv or greater indicate stratospheric air.

Figure 6. Times series of chemical species and DC-8 altitude along Flight 10. Mixing ratios of NO (pptv), NO_y (pptv), CO (ppbv), and O_3 (ppbv) along the flight track are given in the first four panels. The bottom panel indicates the altitude of the DC-8. Chemical signatures are indicated on the top panel (STR-stratospheric, TRS-transition, LT-lightning, and POL-pollution). Lightning events within the transition zone and at the end of the stratospheric leg are indicated with arrows.

Figure 7. Times series of chemical species and DC-8 altitude along Flight 10. Concentrations of ultrafine CN (cm^{-3}) and mixing ratios of PAN (pptv) and H_2O (ppmv) along the flight track are given in the first three panels. The bottom panel indicates the altitude of the DC-8. Chemical signatures are indicated on the top panel (STR-stratospheric, TRS-transition, LT-lightning, and POL-pollution). Lightning events within the transition zone are indicated with arrows.

Figure 8. Cross section of MM5 derived potential vorticity (PVU) through the cut-off low pressure system at 1200 UTC October 29, 1997. Altitude (km) and horizontal distance are indicated. The axis is shown in Figure 3d.

Figure 9. Backward trajectories arriving at LT1 (50-51 hours back). Arrival time at flight level is 1400-1500 UTC October 29, 1997. Arrows along trajectory paths indicate locations at six hour intervals.

Figure 10. Trajectory altitudes (km) as a function of time (hours back) for arrivals at LT1 (1404-1452 UTC).

Figure 11. Backward trajectories arriving at LT3 (53 hours back). Arrival time at flight level is 1700 UTC October 29, 1997. Arrows along trajectory paths indicate locations at six hour intervals.

Figure 12. Backward trajectories arriving at POL (51-53 hours back). Arrival time at flight level is 1500-1700 UTC October 29, 1997. Arrows along trajectory paths indicate trajectory locations at six hour intervals.

Figure 13. Trajectory altitudes (km) as a function of time (hours back) for arrivals at POL (1527-1646 UTC).

Figure 14. Backward trajectories arriving at portion of the transition (TRS) segment (51 hours back). Arrival time at flight level is 1500-1700 UTC October 29,1997. Arrows along trajectory paths indicate locations at six hour intervals.

Figure 15. Trajectory altitudes (km) as a function of time (hours back) for arrivals at the 1453-1526 UTC portion of TRS.

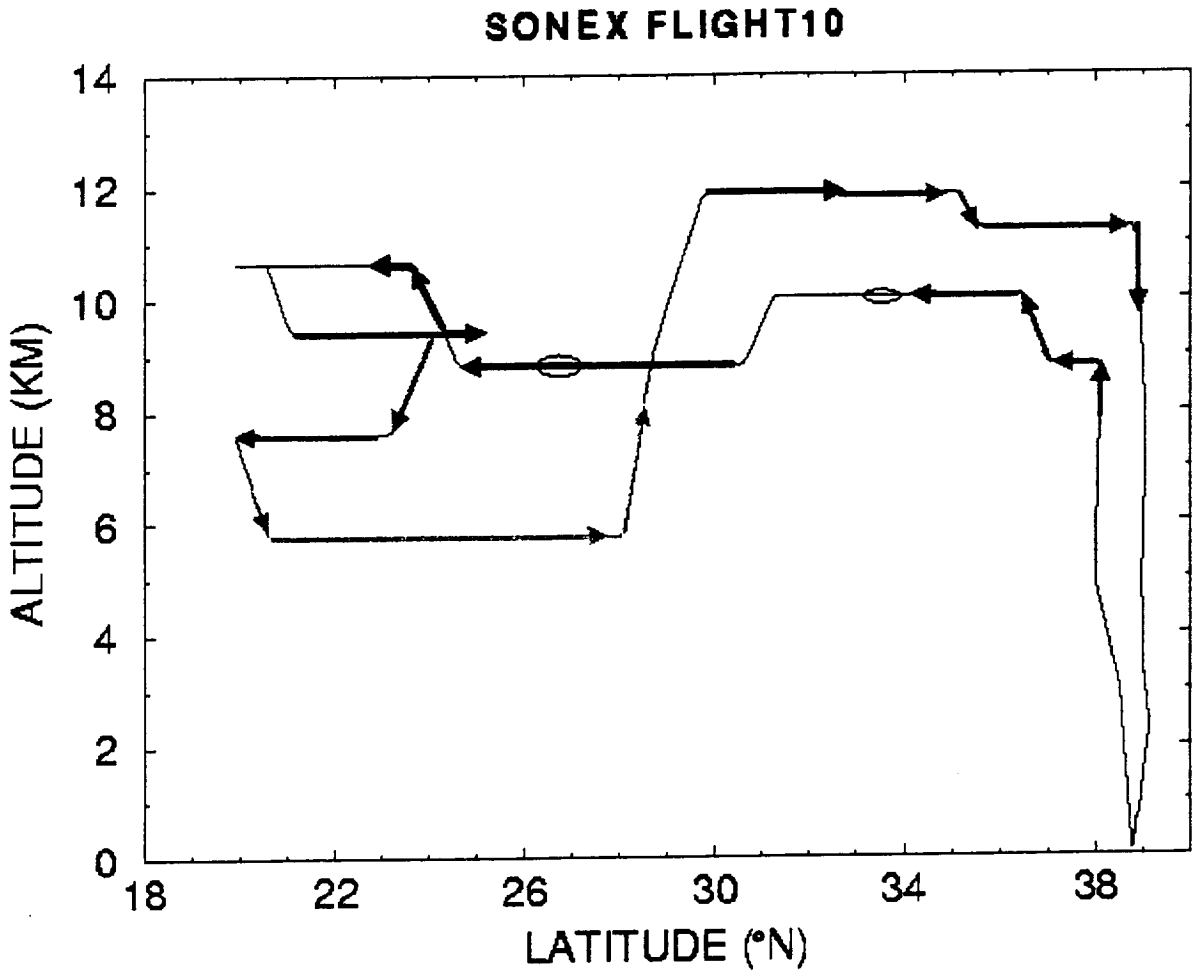

Plate 1. Altitude profile of Flight 10 as a function of latitude. Chemical signatures are indicated by colored segments as follows: Red-stratospheric, blue-lightning, green-transition, and orange-pollution.

Tropical Survey

SONEX Flight 10 29 Oct 97

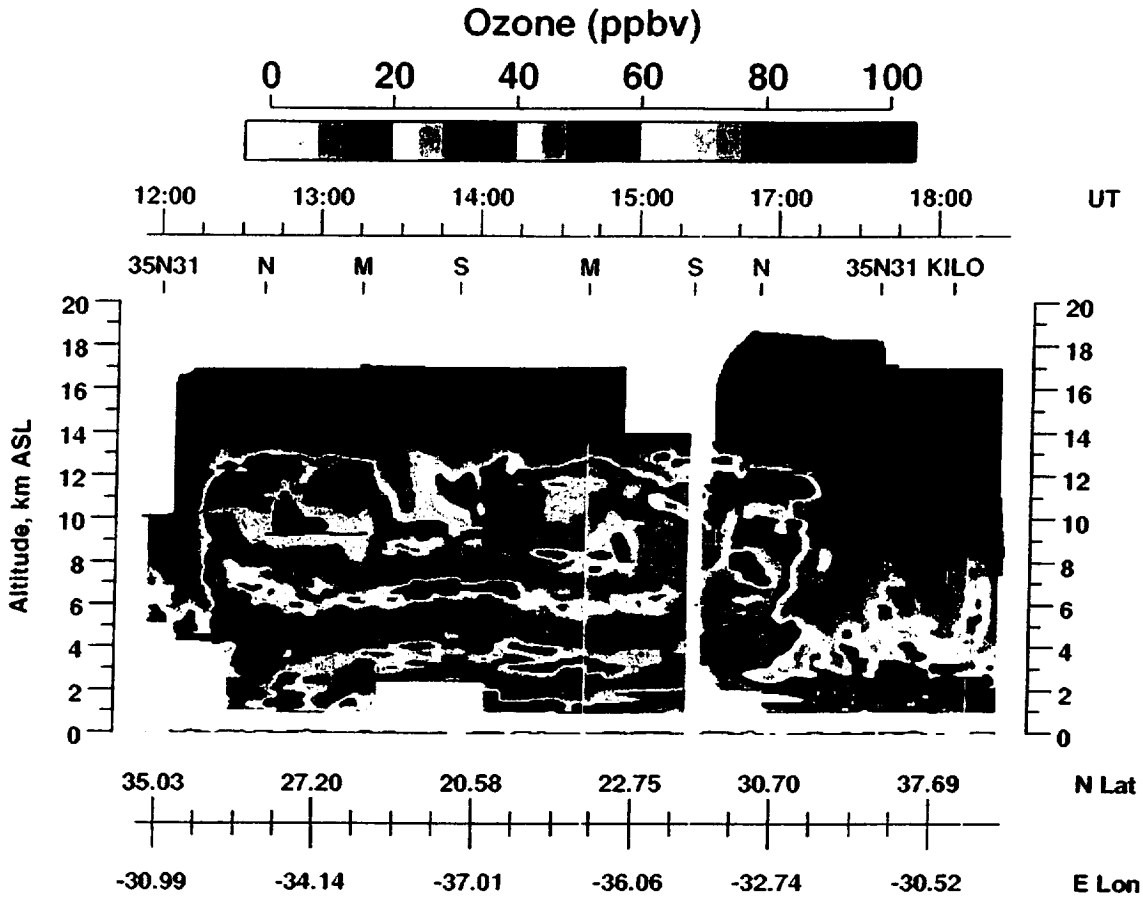

Plate 2. Cross section of DIAL-derived O_3 mixing ratio. The O_3 scale (ppbv) and time (UTC) are give at the top while latitude and longitude are given at the bottom. Altitude in kilometers is given along the sides.

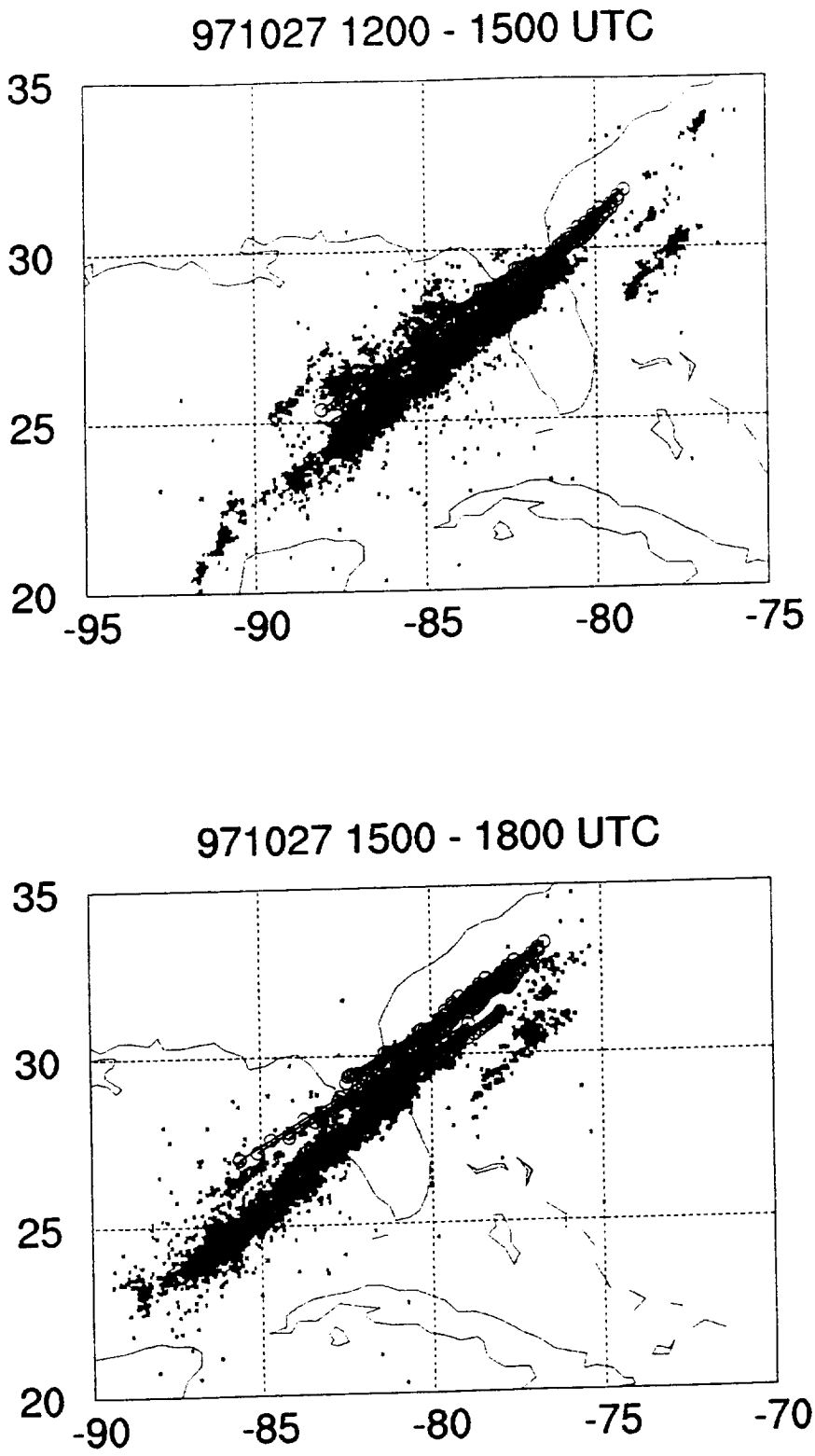

Plate 3. Lightning event 1. Three hour trajectory paths are indicated by blue circles. NLDN cloud-to-ground lightning flashes are indicated in red. The time segment is given at the top of each panel.

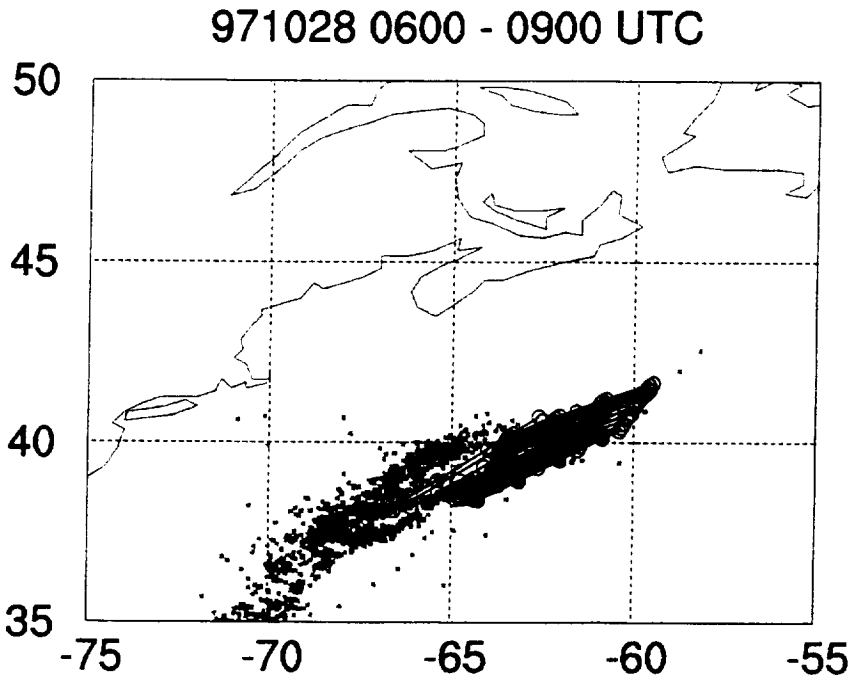

Plate 3. (continued)

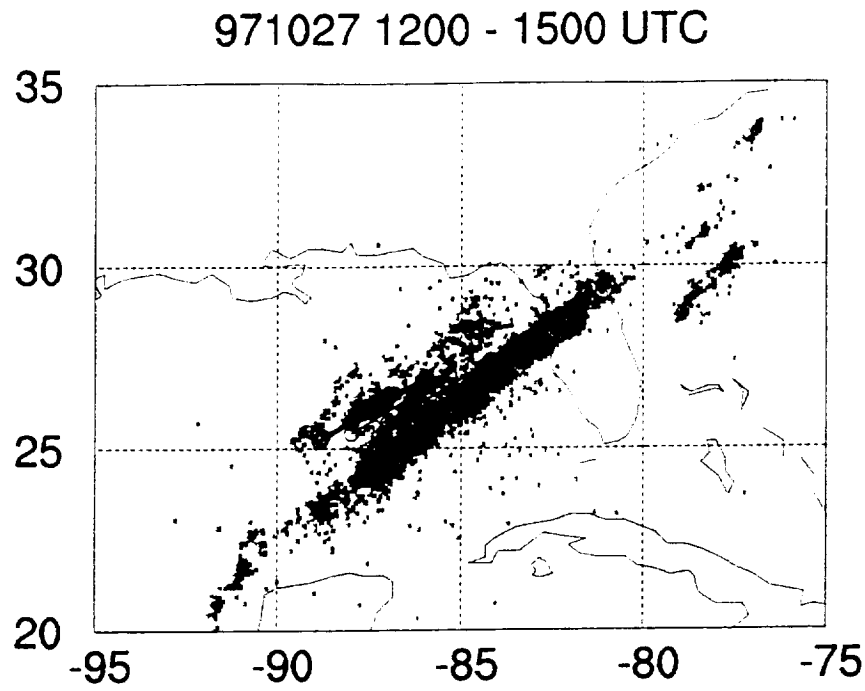

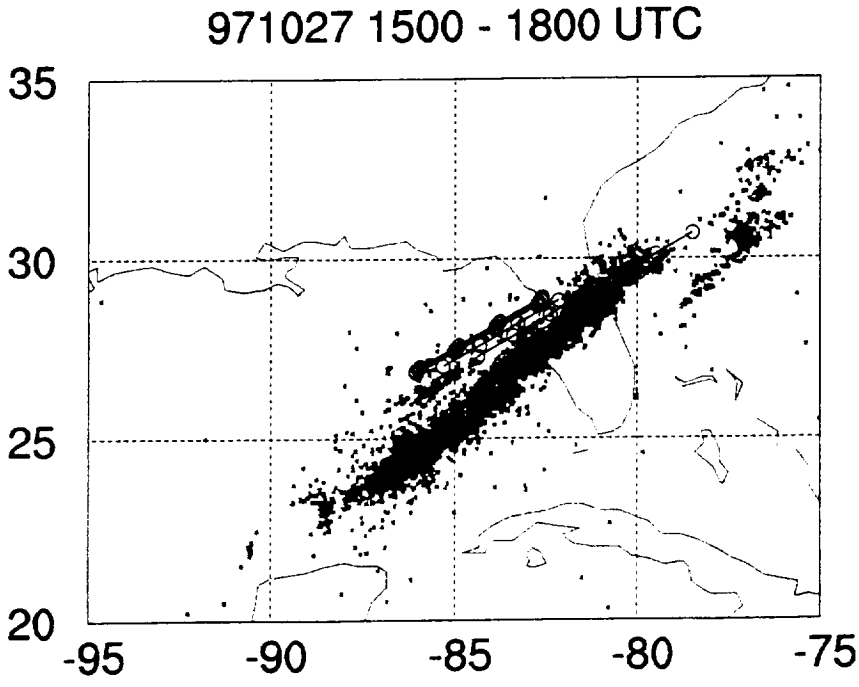

Plate 4. Lightning event 2. Three hour trajectory paths are indicated by blue circles. NLDN cloud-to-ground lightning flashes are indicated in red. The time segment is given at the top of each panel.

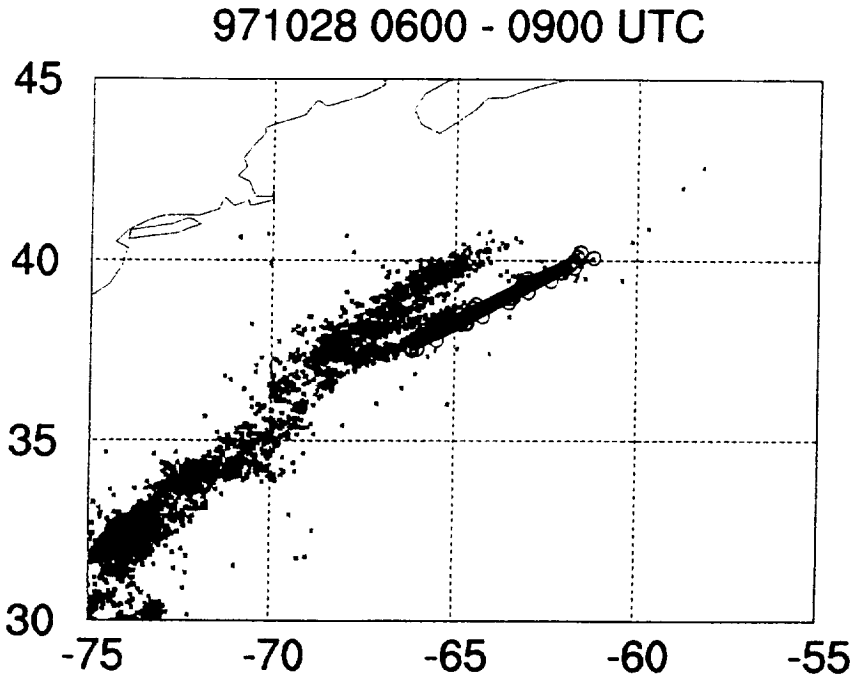

Plate 4. (continued)

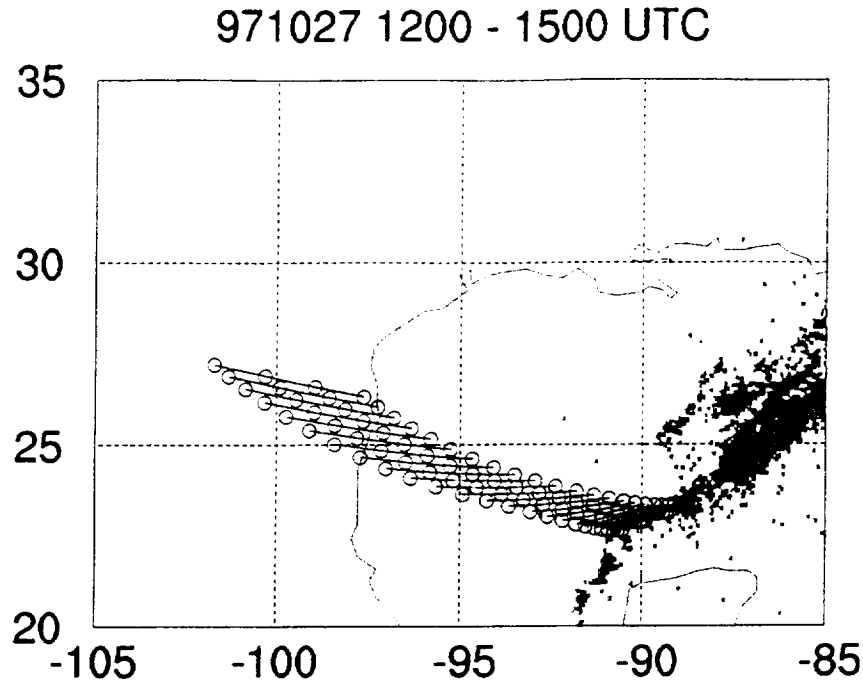

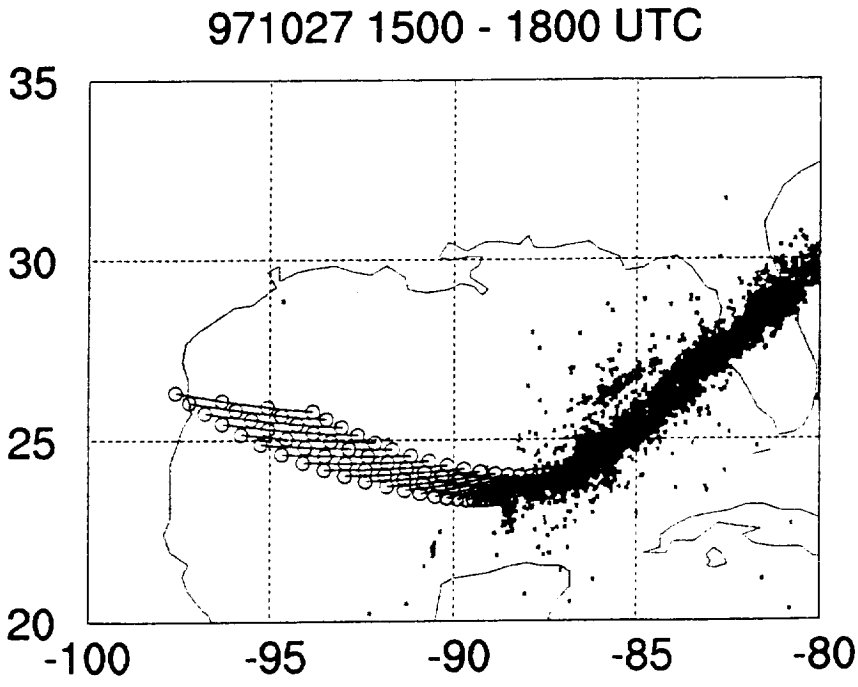

Plate 5. Lightning event 3. Three hour trajectory paths are indicated by blue circles. NLDN cloud-to-ground lightning flashes are indicated in red. The time segment is given at the top of each panel.

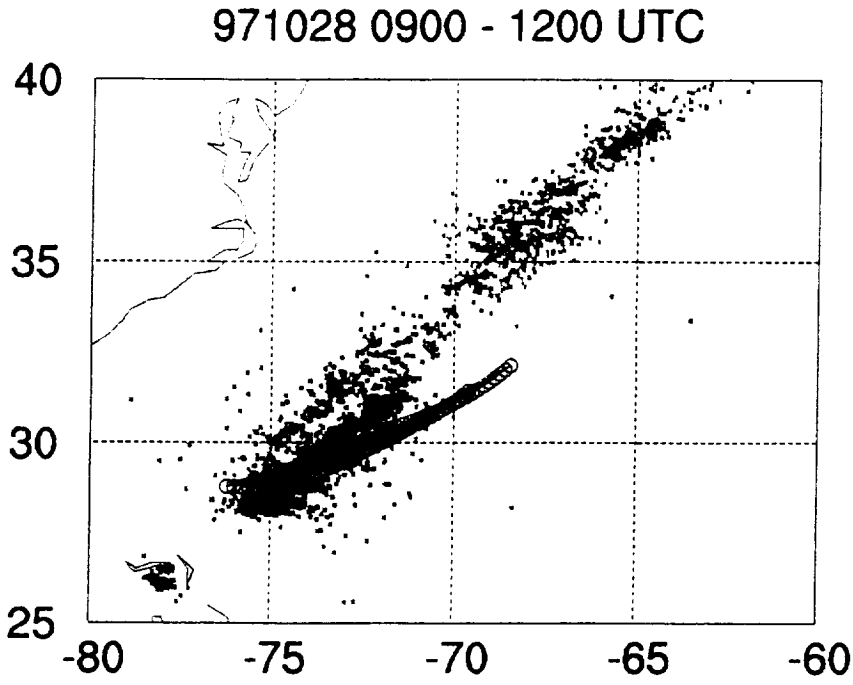

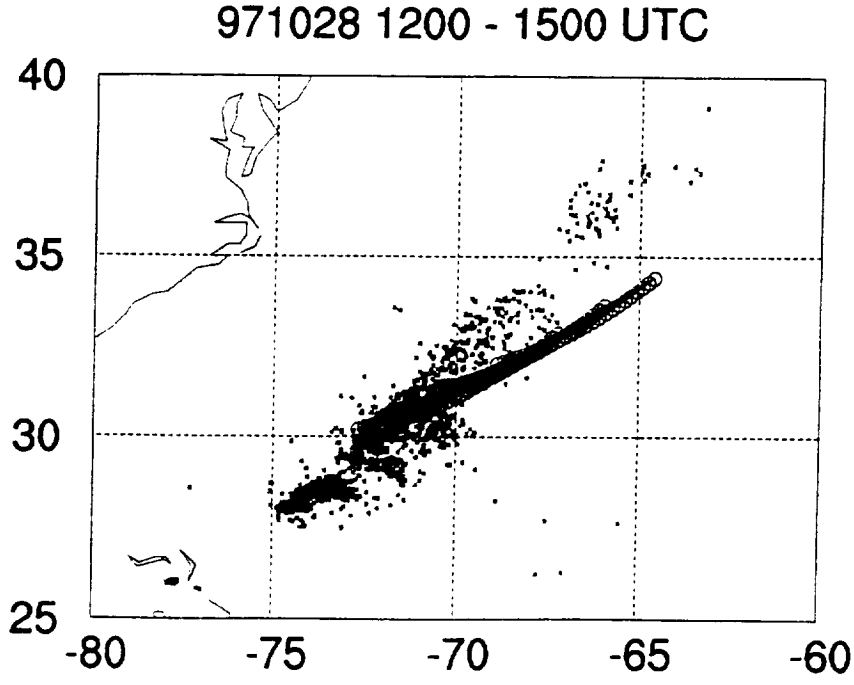

Plate 5. (continued)

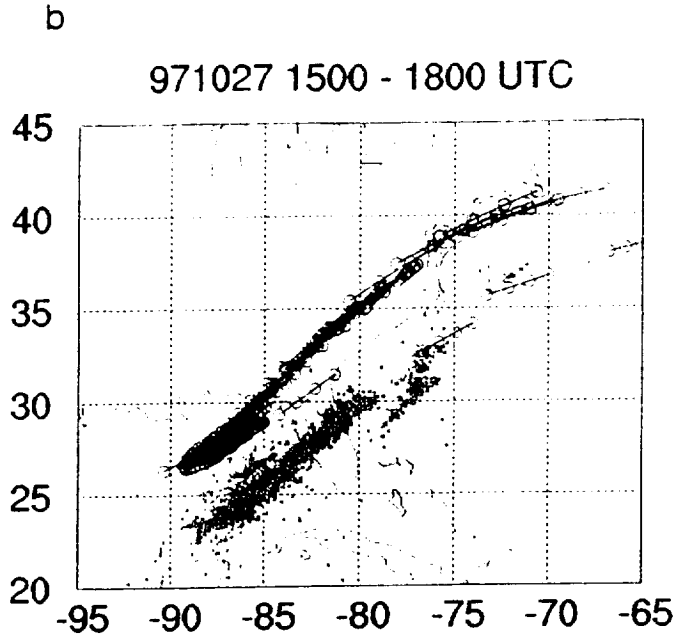

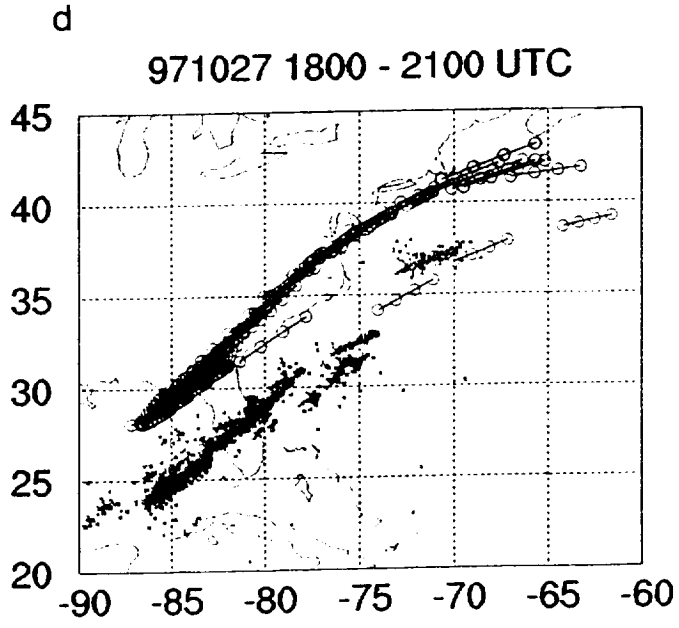

Plate 6. a) GOES-8 infrared satellite image at 1445 UTC October 27, 1997.
b) Three hour trajectory paths (blue) and NLDN cloud-to-ground lightning strikes (red) for the period of 1500-1800 UTC October 27, 1997.
c) GOES-8 infrared satellite image at 2045 October 27, 1997.
d) Three hour trajectory paths (blue) and NLDN cloud-to-ground lightning strikes (red) for the period of 1800-2100 UTC October 27, 1997.

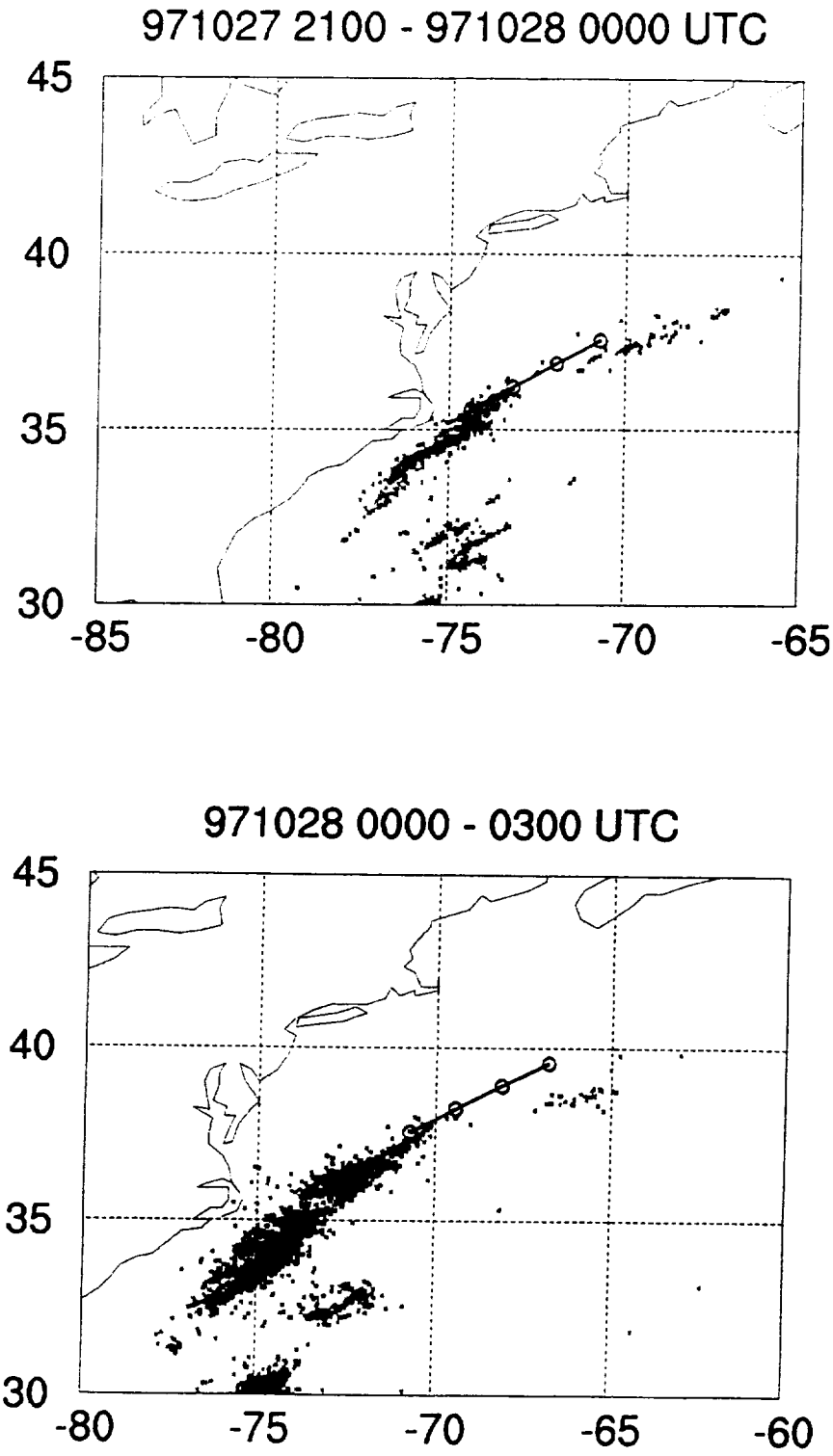

Plate 7. Transitional segment. Three hour trajectory paths are indicated by blue circles. NLDN cloud-to-ground lightning flashes are indicated in red. The time segment is given at the top of each panel.

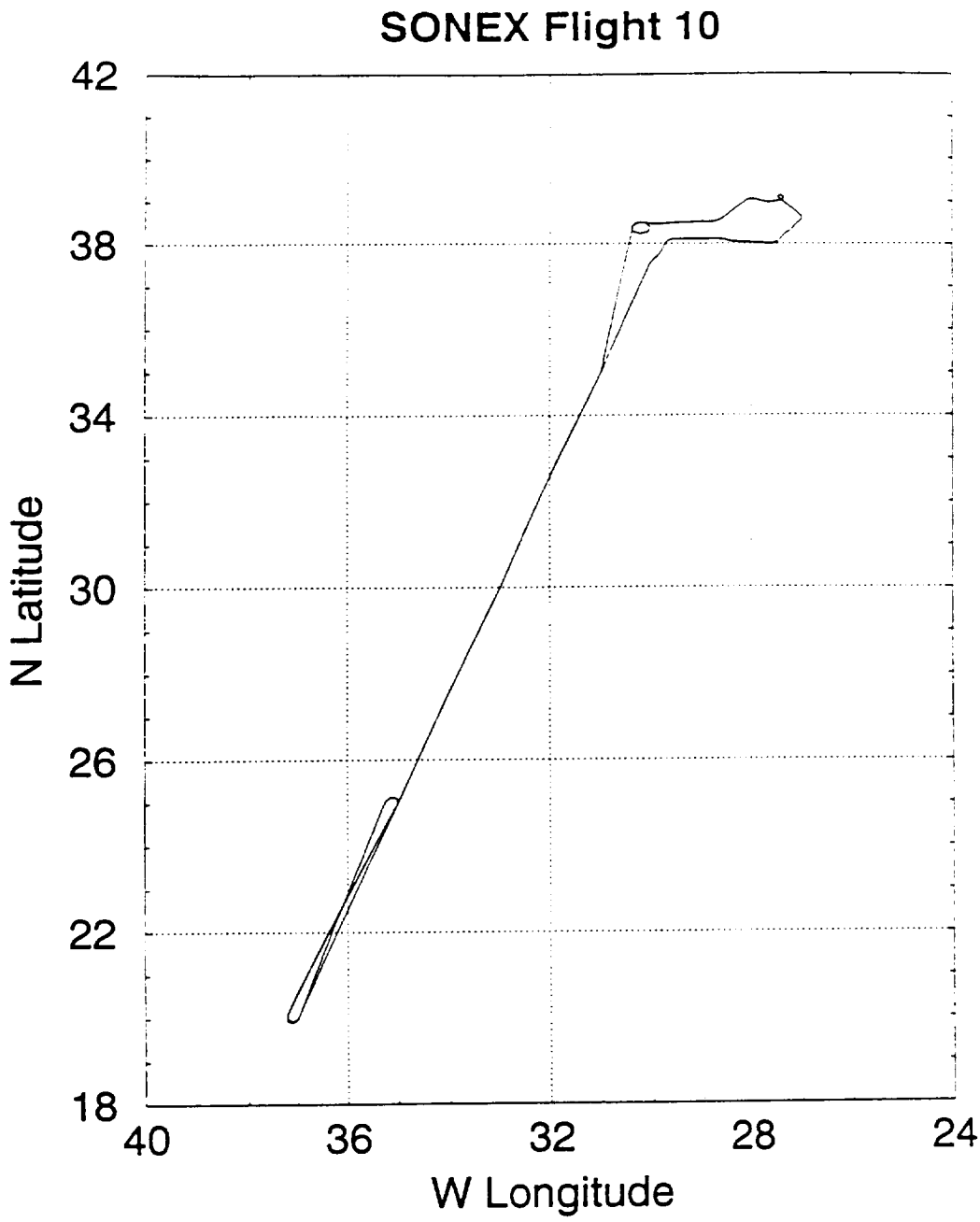

Figure 1. DC-8 flight track on October 29, 1997.

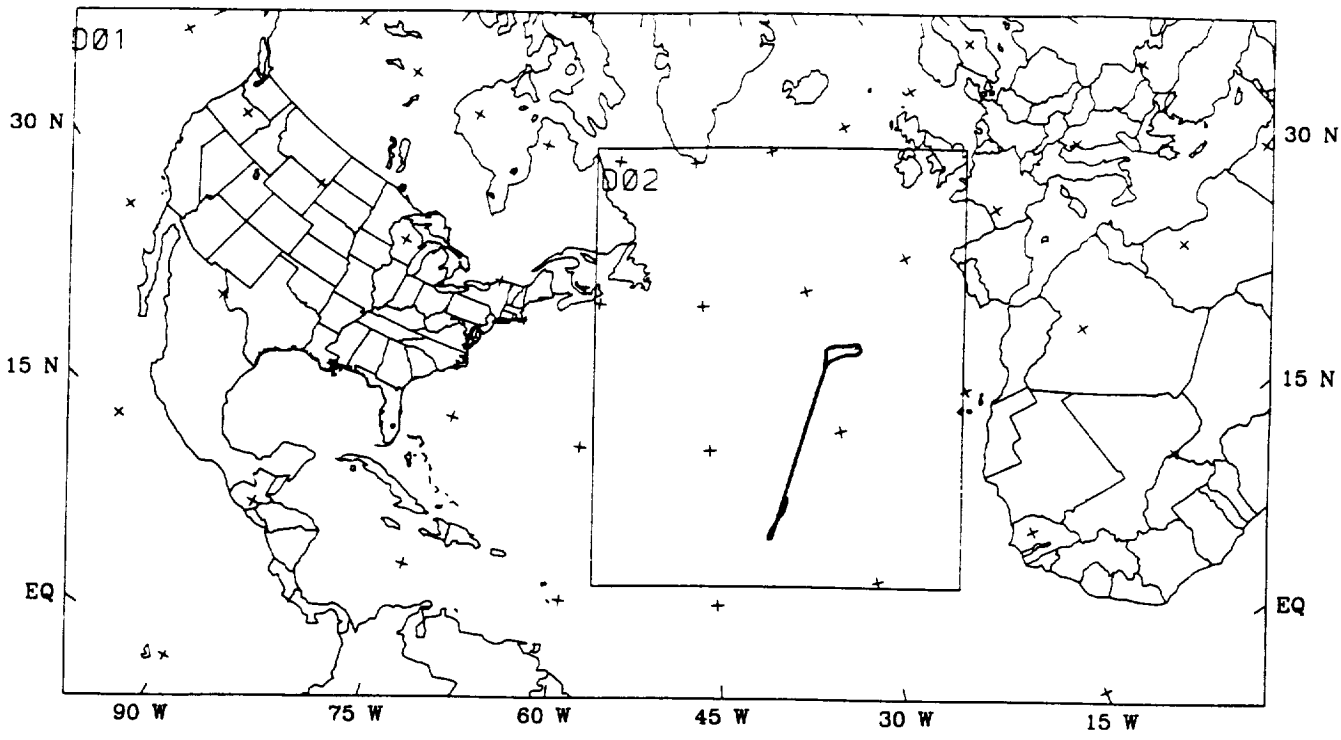

Figure 2. Domains for the MM5 simulation. The outer perimeter indicates the boundary of the 90 km domain. The inner box represents the area of the 30 km domain. The track of Flight 10 is indicated within the 30 km domain.

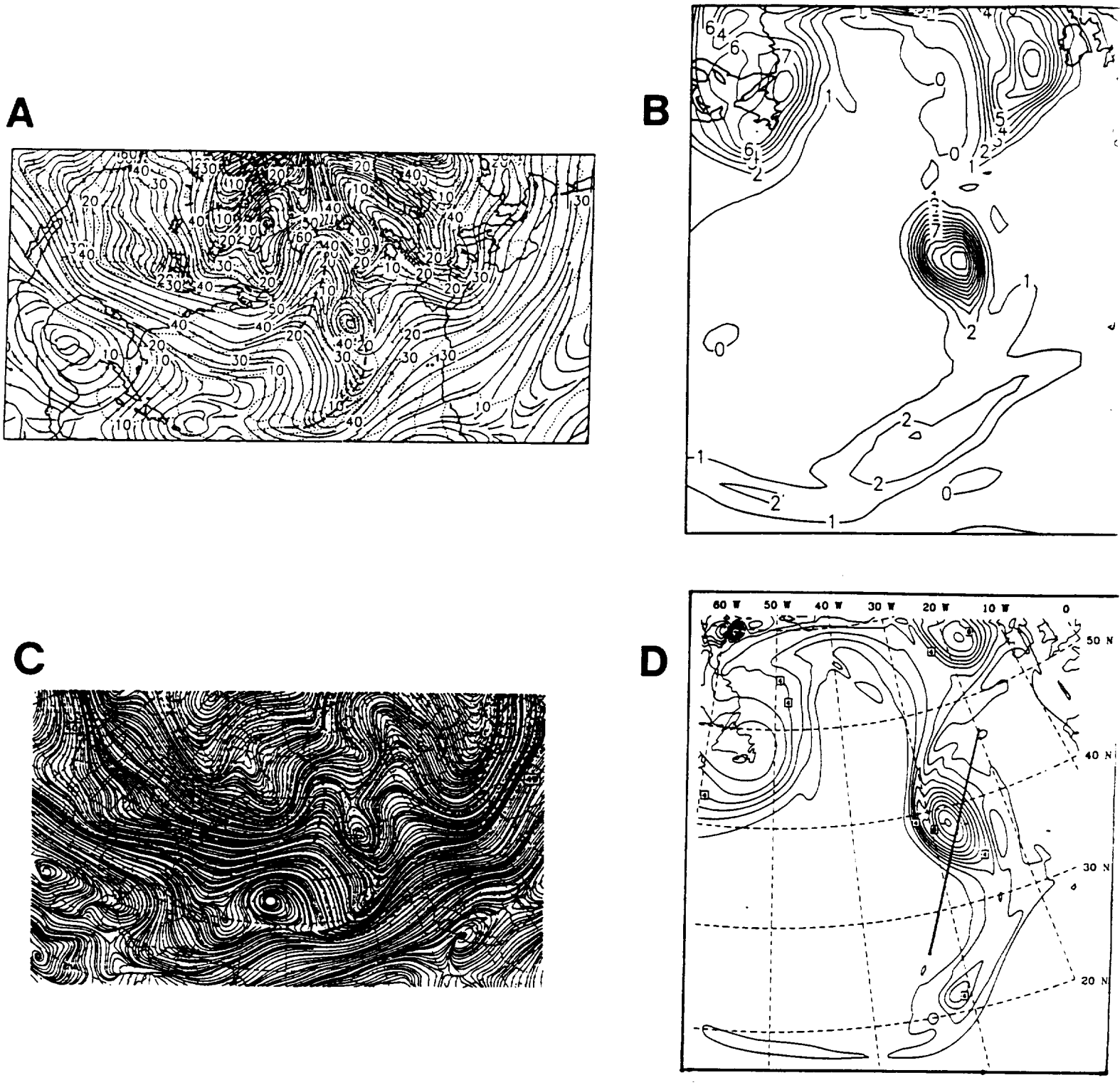

Figure 3. a) ECMWF 250 hPa streamlines and isotachs at 1200 UTC October 29, 1997. Wind speeds are contoured at intervals of 10 m s^{-1}.

b) ECMWF 250 hPa potential vorticity at 1200 UTC October 29, 1997. Contours are 1 PVU.

c) MM5 250 hPa streamlines and isotachs at 1200 UTC October 29, 1997. Wind speeds are contoured at intervals of 10 m s^{-1}.

d) MM5 250 hPa potential vorticity at 1200 UTC October 29, 1997. Contours are 1 PVU. The axis of a cross section in Figure 8 is shown.

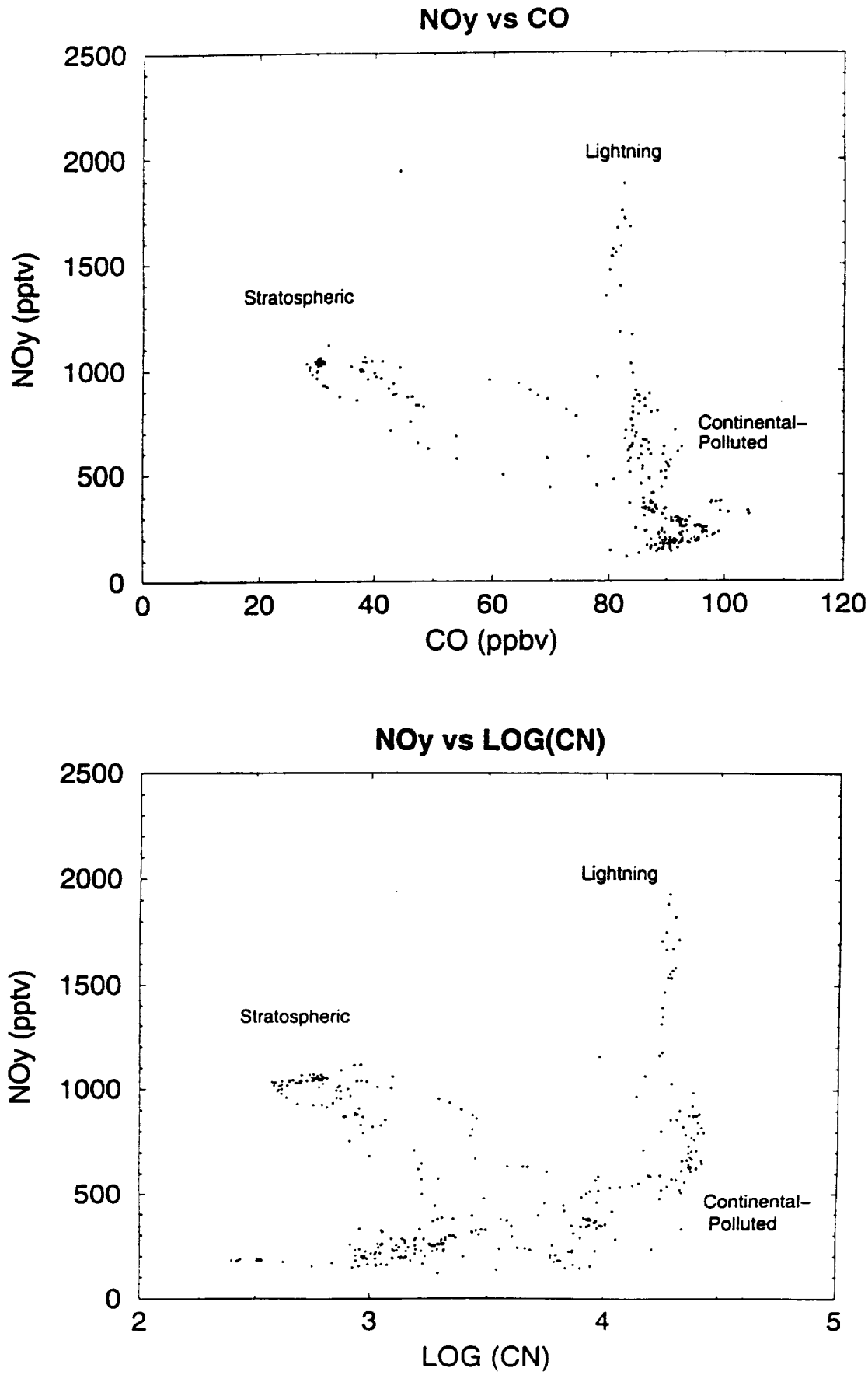

Figure 4. a) Correlation plot of NO_y (pptv) versus CO (ppbv). The three main signatures of Flight 10 are labeled.

b) Correlation plot of NO_y (pptv) versus the logarithm of ultrafine CN (cm^{-3}). The three main signatures of Flight 10 are labeled.

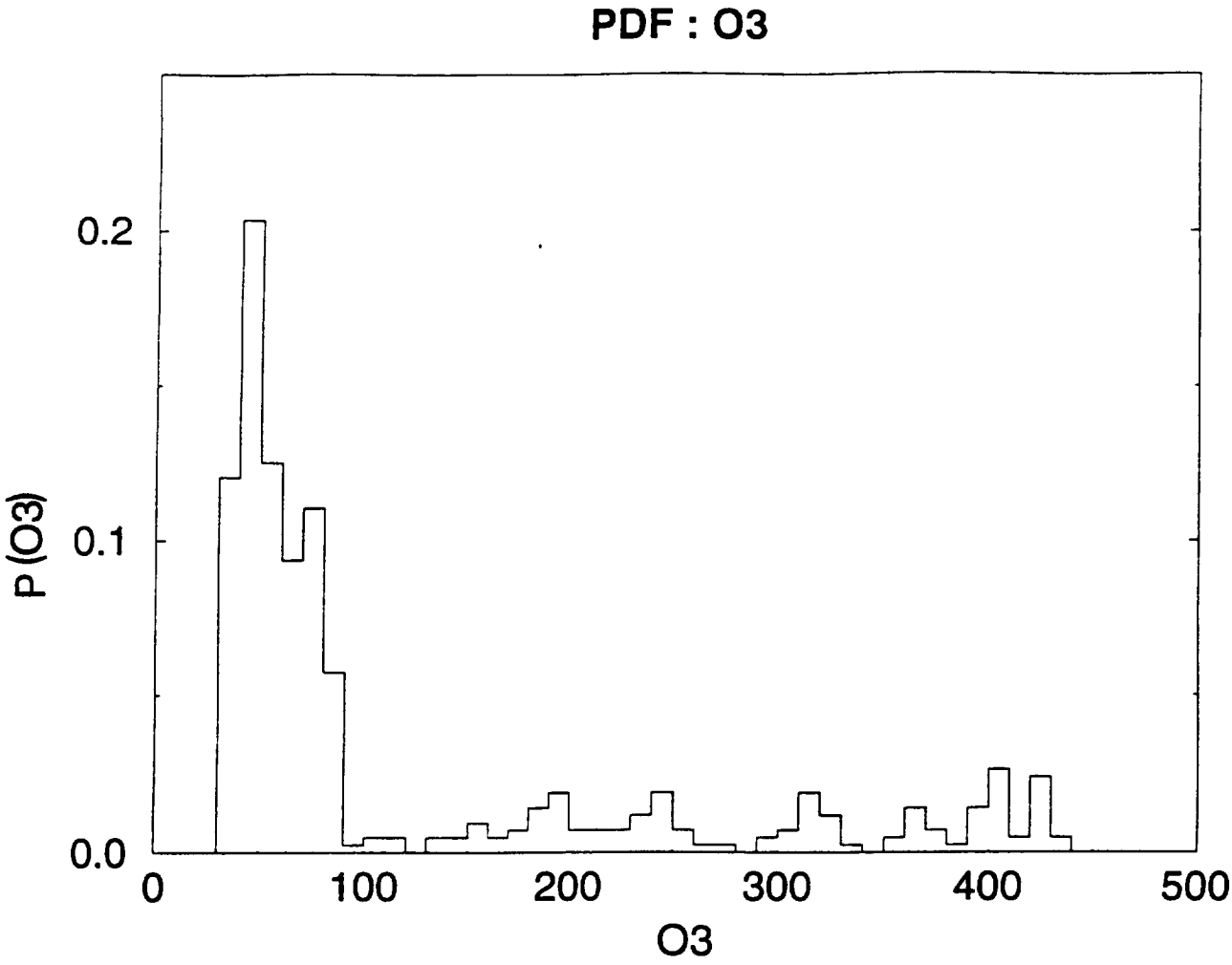

Figure 5. Probability distribution function of O_3 for Flight 10. Ozone values of 100 ppbv or greater indicate stratospheric influence.

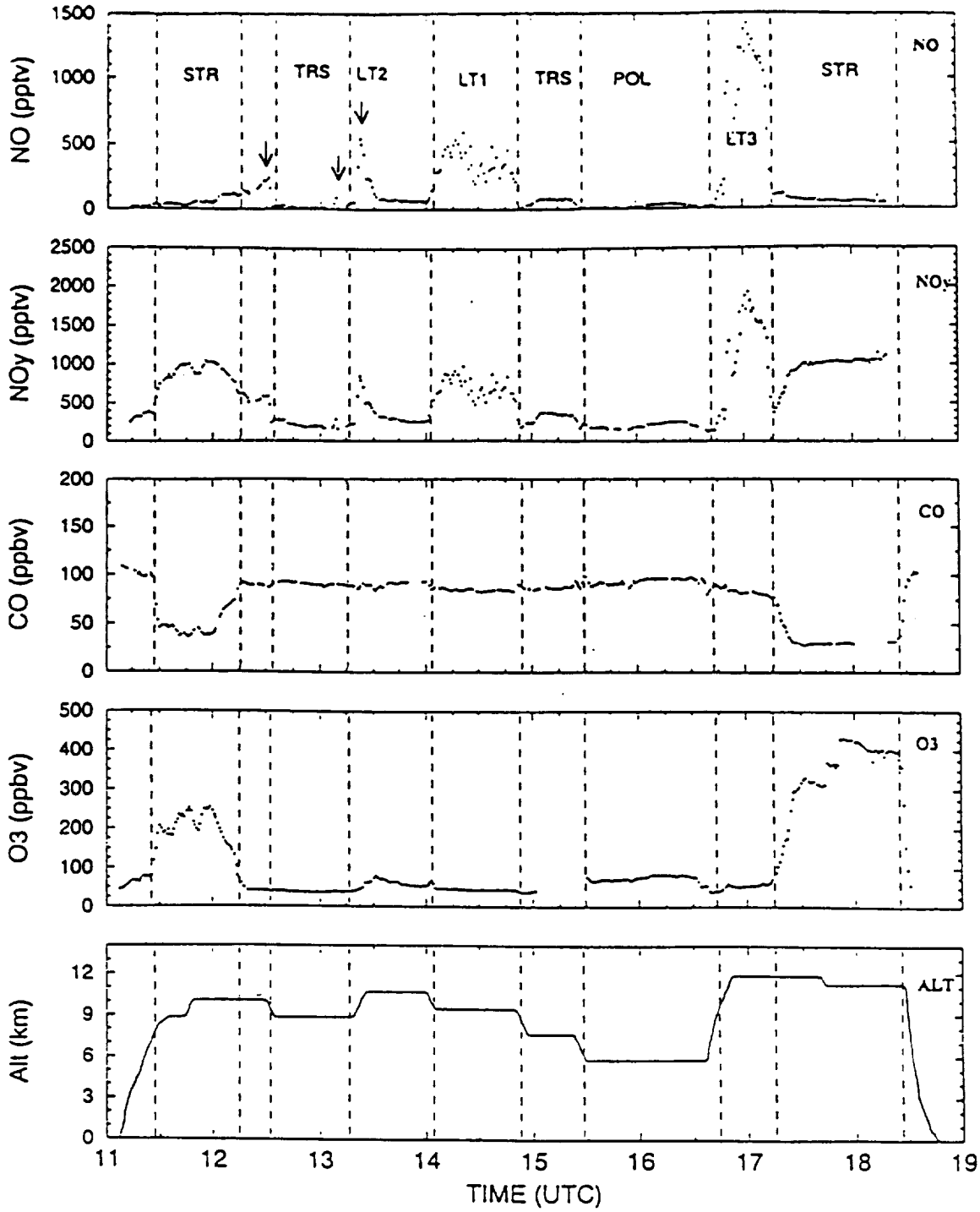

Figure 6. Time series of chemical species and DC-8 altitude along Flight 10. Mixing ratios of NO (pptv), NO_y (pptv), CO (ppbv), and O_3 (ppbv) along the flight track are given in the first four panels. The bottom panel indicates the altitude of the DC-8. Chemical signatures are indicated on the top panel (STR-stratospheric, TRS-transition, LT-lightning, and POL-pollution). Lightning events within the transition zone and at the end of the stratospheric leg are indicated with arrows.

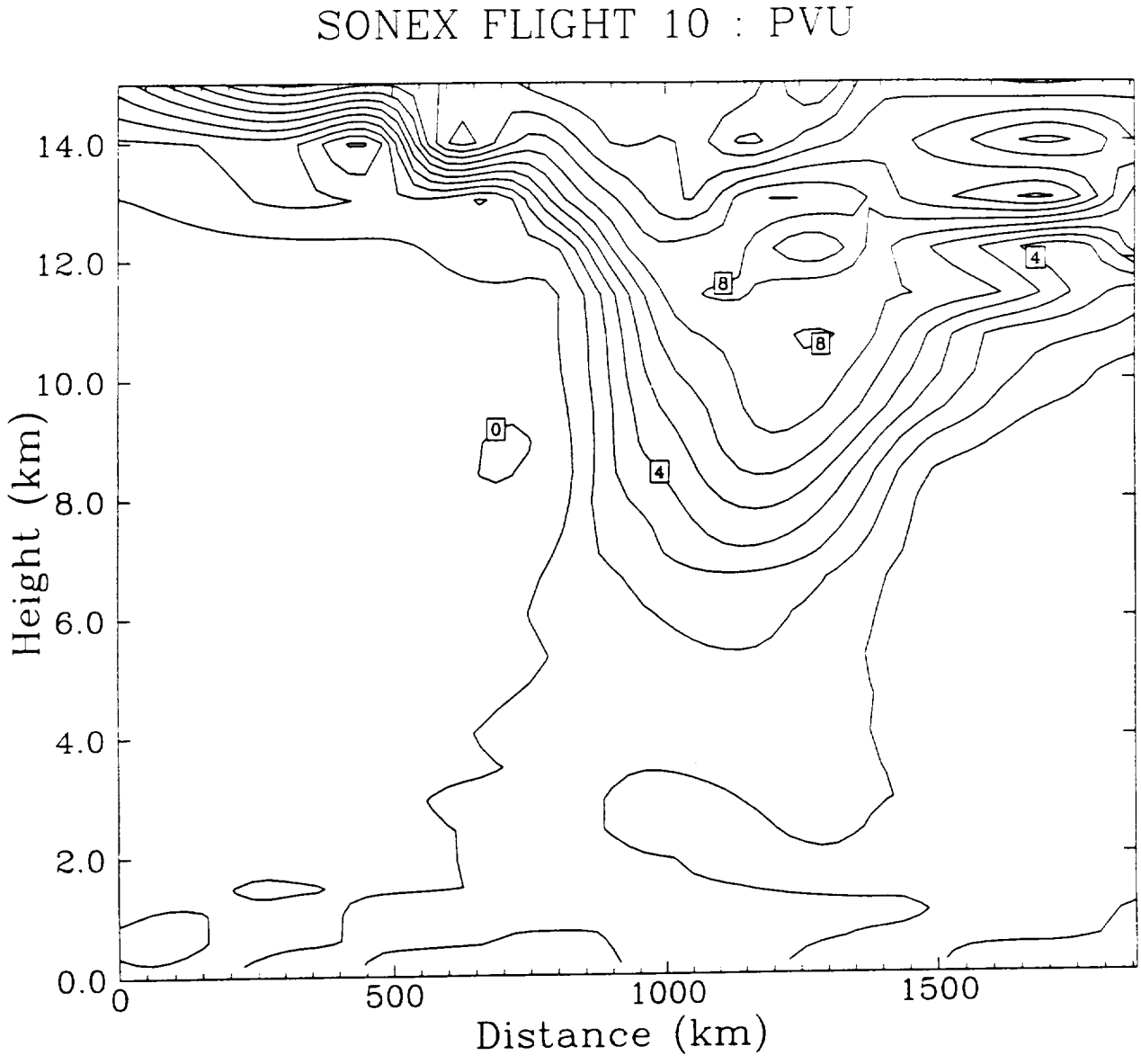

Figure 8. Cross section of MM5 derived potential vorticity (PVU) through the cut-off low pressure system at 1200 UTC October 29, 1997. Altitude (km) and horizontal distance are indicated. The axis is shown in Figure 3d.

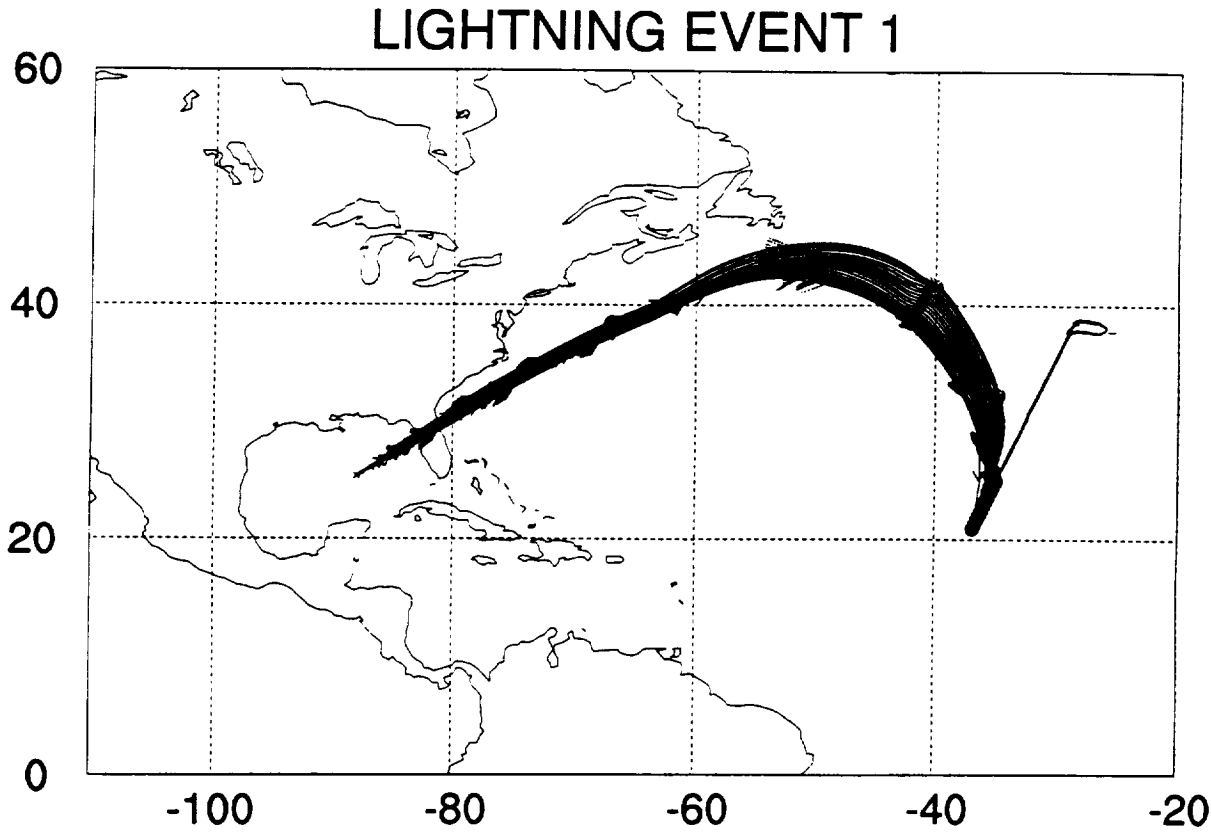

Figure 9. Backward trajectories arriving at LT1 (50-51 hours back). Arrival time at flight level is 1400-1500 UTC October 29, 1997. Arrows along trajectory paths indicate locations at six hour intervals.

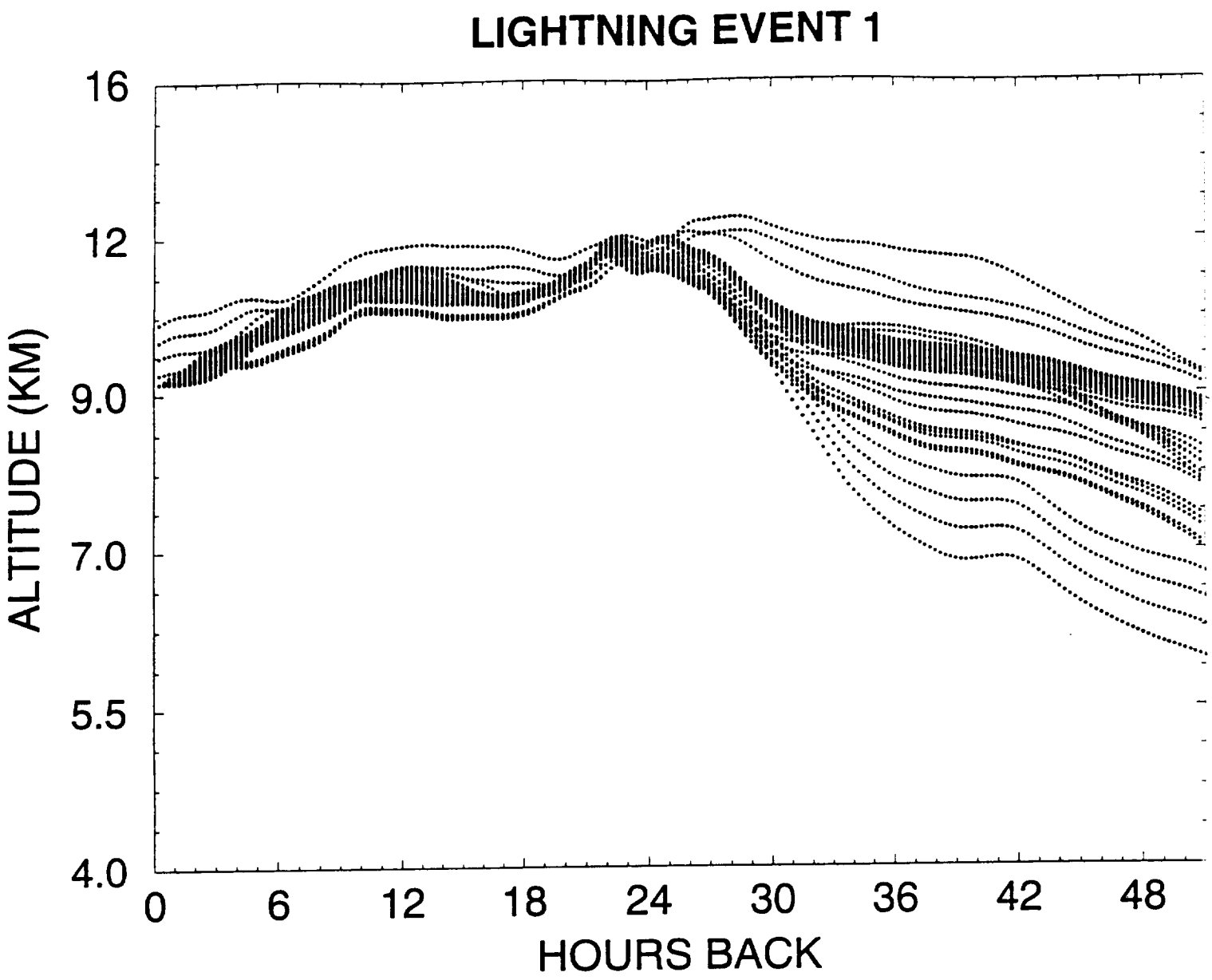

Figure 10. Trajectory altitudes (km) as a function of time (hours back) for arrivals at LT1.

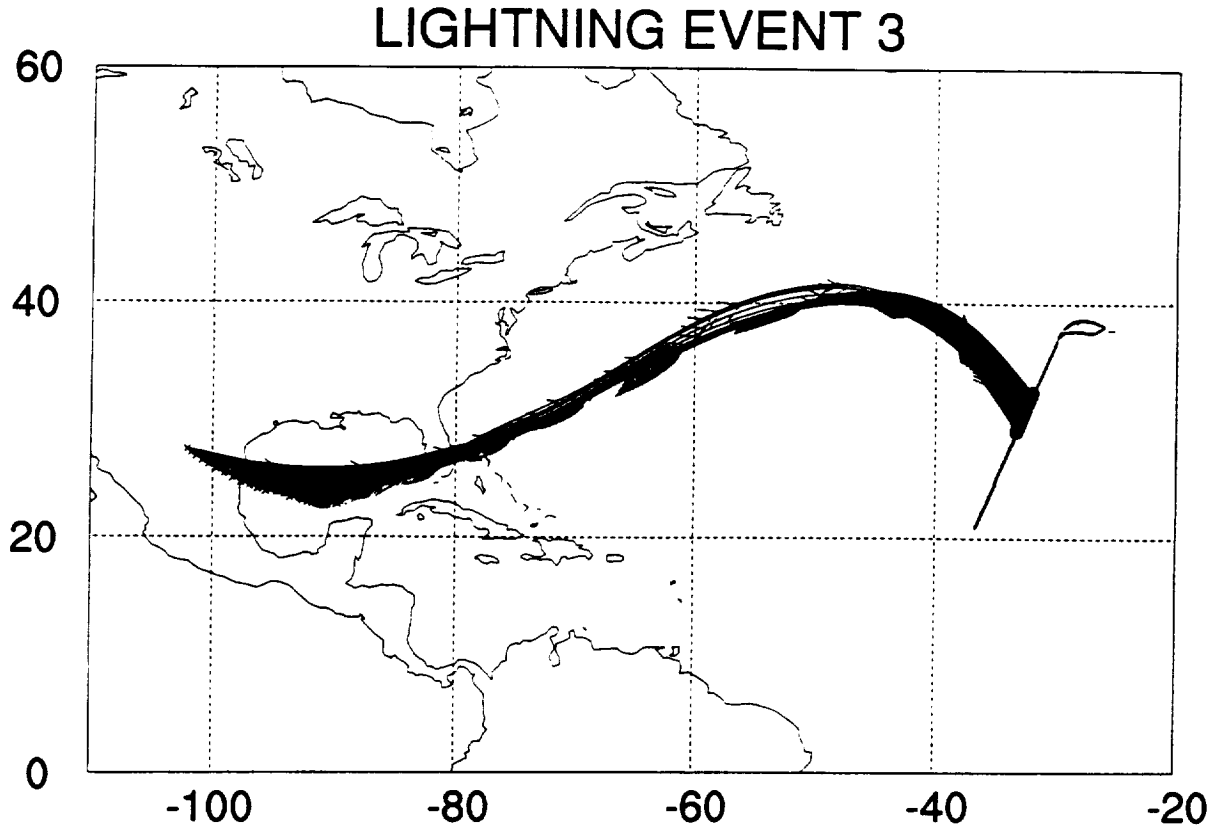

Figure 11. Backward trajectories arriving at LT3 (53 hours back). Arrival time at flight level is 1700 UTC October 29, 1997. Arrows along trajectory paths indicate locations at six hour intervals.

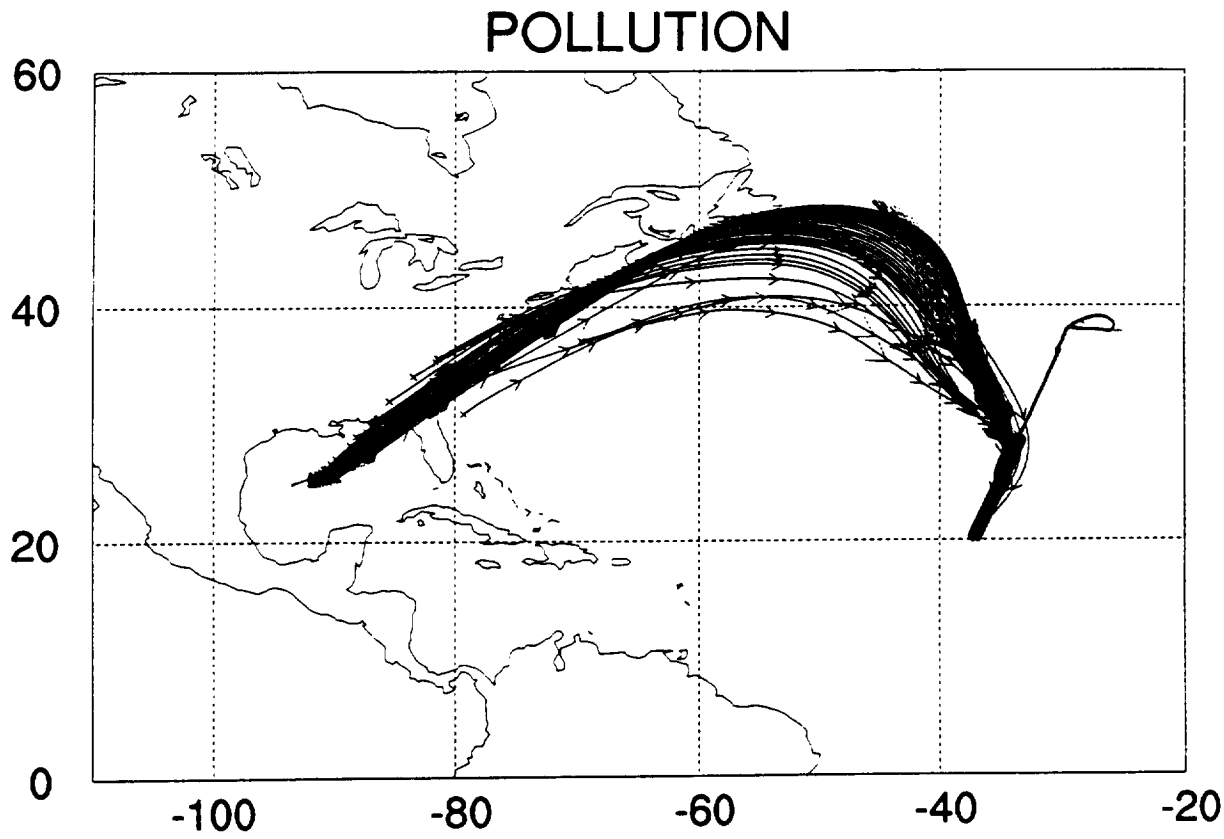

Figure 12. Backward trajectories arriving at POL (51-53 hours back). Arrival time at flight level is 1500-1700 UTC October 29, 1997. Arrows along trajectory paths indicate trajectory locations at six hour intervals.

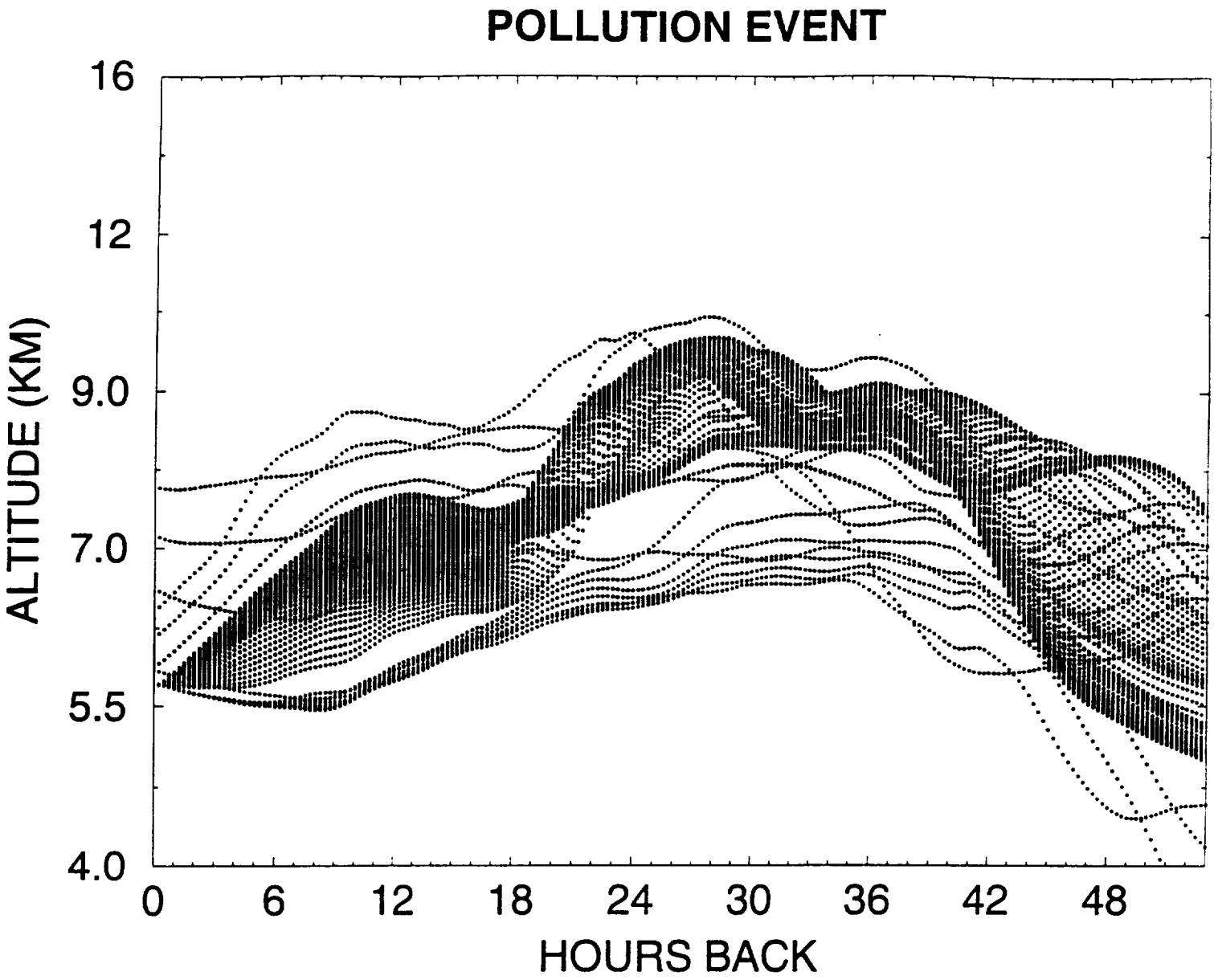

Figure 13. Trajectory altitudes (km) as a function of time (hours back) for arrivals at POL.

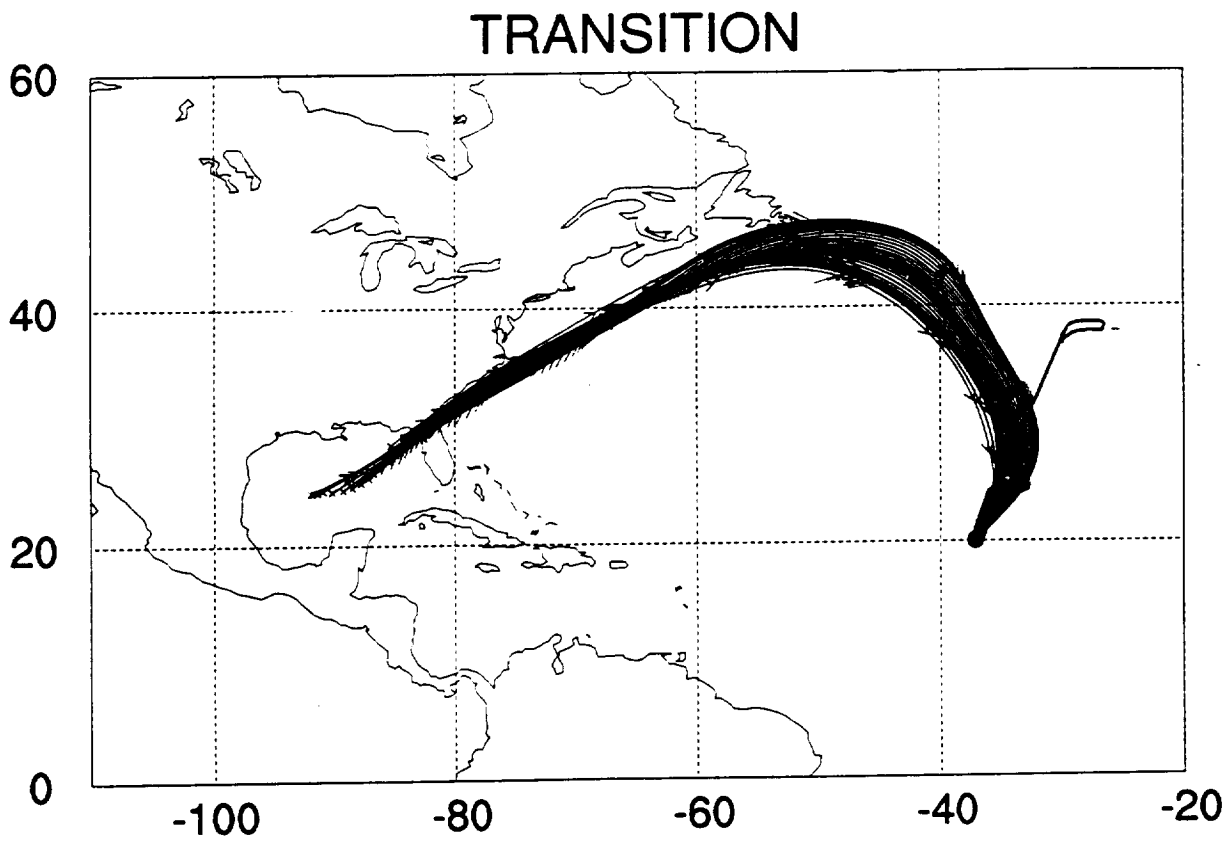

Figure 14. Backward trajectories arriving at portion of the transition (TRS) segment (51 hours back). Arrival time at flight level is 1500-1700 UTC October 29,1997. Arrows along trajectory paths indicate locations at six hour intervals.

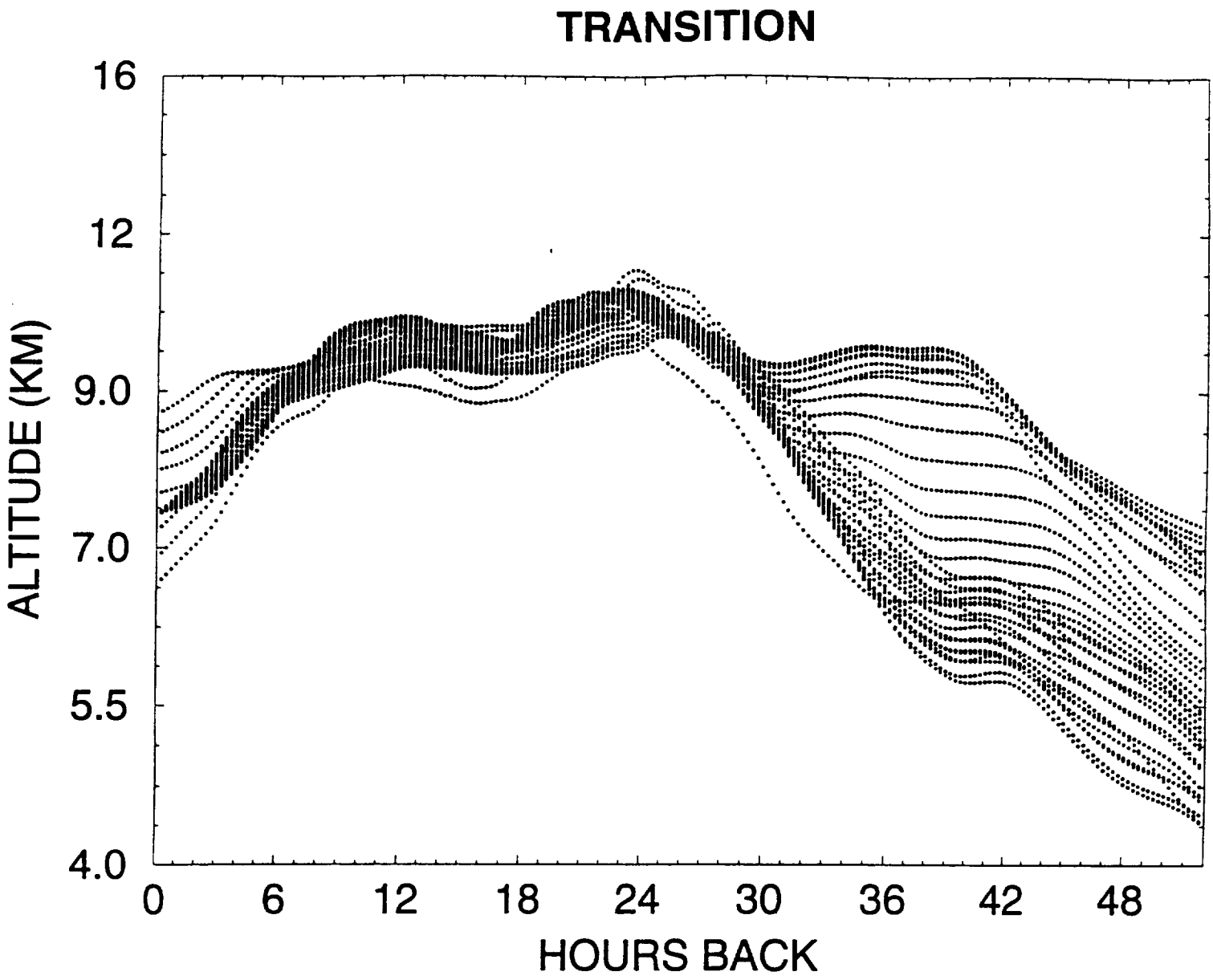

Figure 15. Trajectory altitudes (km) as a function of time (hours back) for arrivals at TRS.